frontiers | Frontiers in Plant Science

TYPE Original Research
PUBLISHED 12 December 2025
DOI 10.3389/fpls.2025.1708928

Check for updates

OPEN ACCESS

EDITED BY
Sandeep Singh,
Punjab Agricultural University, India

REVIEWED BY
Xiaoming Wang,
Northwest A&F University, China
Pawandeep Singh Kohli,
Institute of Plant Sciences, Switzerland

*CORRESPONDENCE
Benjamin Stich
Benjamin.Stich@julius-kuehn.de

†Deceased

RECEIVED 19 September 2025
REVISED 06 November 2025
ACCEPTED 10 November 2025
PUBLISHED 12 December 2025

CITATION
Rouina H, Singh D, Arlt C, Malekian B, Schreiber L, Stich B and Marshall-Colon A (2025) Regulatory analysis of root architectural and anatomical adaptation to nitrate and ammonium in *Brachypodium distachyon*. *Front. Plant Sci.* 16:1708928. doi: 10.3389/fpls.2025.1708928

COPYRIGHT
© 2025 Rouina, Singh, Arlt, Malekian, Schreiber, Stich and Marshall-Colon. This is an open-access article distributed under the terms of the Creative Commons Attribution License (CC BY). The use, distribution or reproduction in other forums is permitted, provided the original author(s) and the copyright owner(s) are credited and that the original publication in this journal is cited, in accordance with accepted academic practice. No use, distribution or reproduction is permitted which does not comply with these terms.

Regulatory analysis of root architectural and anatomical adaptation to nitrate and ammonium in *Brachypodium distachyon*

Hamid Rouina[1,2], Dilkaran Singh[3], Christopher Arlt[4,5], Babak Malekian[6], Lukas Schreiber[7], Benjamin Stich[5,8]* and Amy Marshall-Colon[3†]

[1]Forschungszentrum Jülich GmbH, Institute of Bio- and Geosciences, IBG-2: Plant Sciences, Jülich, Germany, [2]Faculty of Agriculture, University of Bonn, Bonn, Germany, [3]Department of Plant Biology, University of Illinois at Urbana–Champaign, Urbana-Champaign, IL, United States, [4]Quantitative Genetik & Genomik der Pflanzen, Heinrich-Heine-Universität Düsseldorf, Düsseldorf, Germany, [5]Julius Kühn Institute, Federal Research Centre on Cultivated Plants, Institute for Breeding Research on Agricultural Crops, Sanitz, Germany, [6]Department of Forest and Soil Sciences, Institute of Forest Ecology, University of Natural Resources and Life Sciences (BOKU), Vienna, Austria, [7]Institute of Cellular and Molecular Botany, University of Bonn, Bonn, Germany, [8]Faculty of Agricultural and Environmental Sciences, University of Rostock, Rostock, Germany

Plants deploy different strategies to optimize the nitrogen (N) uptake via roots, based on a complicated regulatory network that controls root phenotype and physiology. Here, we studied the response of root architecture to varying N applications in the model species *Brachypodium distachyon*. Using a combination of phenotypic and transcriptomic analyses, we examined how different forms and concentrations of ammonium and nitrate affect root growth, biomass allocation, and N uptake. N concentrations significantly influenced root traits such as root length, root hair development, and aerenchyma formation in response to nitrate and ammonium. Plants grown in ammonium conditions had thin but highly branched roots, whereas nitrate application resulted in shorter, thicker roots with denser root hair at higher nitrate concentrations. Furthermore, using co-expression network analysis, we identified an Atypical Aspartic Protease (*APs*) gene encoding an aspartyl protease family protein and a phosphoenolpyruvate carboxylase 1 (*PEPC1*) gene in Brachypodium as potential regulators. Both genes have previously not been associated with N-form-specific root architectural and anatomical adaptions in Brachypodium. *APs* expression showed a positive correlation with total root length and lateral root development, along with a negative correlation with root hair density. In contrast, *PEPC1* exhibited positive correlations with cortex, stele, root cross-sectional areas, and root hair density, while showing a negative

correlation with total root length. Our findings provide new insights into the molecular mechanisms underlying N-form-specific root adaptation and highlight the functional plasticity of root systems in response to environmental nutrient cues laying the groundwork for targeted manipulation of root traits in other crops.

KEYWORDS

nitrogen uptake, root architecture, *Brachypodium distachyon*, transcriptomic analysis, ammonium and nitrate adaptation

Introduction

Nitrogen (N) uptake by plant roots is dependent on the interplay among root physiological, morphological, anatomical, and transcriptional phenotypes (Liu et al., 2015; Rogers and Benfey, 2015). The study of the genetic mechanisms underlying N uptake is challenging, partly due to the difficulty of root phenotyping caused by limited accessibility, as well as the influence of soil heterogeneity and other environmental factors (Comas et al., 2013; Pereira et al., 2021). However, the critical and adaptive roles of roots in responding to different N applications cannot be overlooked. Although N application responses vary among crop species, most of the root architectural and anatomical traits show genetically conserved responses (Jia and von Wirén, 2020). Nevertheless, compared to the model plant Arabidopsis there is still a considerable gap in knowledge regarding the detailed mechanisms in crop species.

To maximize yield under unfavorable environmental conditions, plants employ dynamic resource allocation strategies as adaptive mechanisms in response to stress. Strategies to improve N uptake efficiency often suggest modifying root architecture, such as developing deeper roots or reducing crown root number in maize to optimize resource uptake under low N conditions (Mi et al., 2010; Saengwilai et al., 2014b; Trachsel et al., 2013). In species like Brachypodium and rice, research indicates that N availability influences root traits and biomass allocation (Jian-Bo et al., 2010; Poiré et al., 2014). In addition, in maize, research indicated that N deficiency enhances water and nutrient absorption efficiency, increases carbon allocation to roots and accelerates root growth (Gaudin et al., 2011; Xiaoli et al., 2020). Also, other anatomical adaptations, such as cortical aerenchyma and larger metaxylem, positively contribute to N acquisition by reducing metabolic costs and enhancing nutrient uptake (Klein et al., 2020; Saengwilai et al., 2014a). It has been demonstrated that the living cells within the cortex of the root segment are responsible for substantially affecting the maintenance cost of the root biomass in general (Jaramillo et al., 2013; Saengwilai et al., 2014a). The development of aerenchyma in roots, a response observed across several species like Brachypodium, wheat, and maize, reduces metabolic demand and aids in nutrient acquisition under low N conditions (Drew et al., 1989; Khan et al., 2015; McDonald et al., 2002). This synergistic interaction between root architectural and anatomical characteristics is an essential strategy of N acquisition (Galindo-Castañeda et al., 2022).

Studies of the root transcriptome in Brachypodium as a model plant for monocot crops demonstrated that carbon metabolism in roots is tightly regulated to support N assimilation, with specific enzymes like phosphoenolpyruvate carboxylase (PEPC) playing crucial roles in balancing carbon and N metabolism (Caburatan and Park, 2021; de la Peña et al., 2019; Nimmo, 2006; Shi et al., 2015). PEPC catalyzes the irreversible carboxylation of phosphoenolpyruvate (PEP) to oxaloacetate, providing carbon skeletons that replenish tricarboxylic acid (TCA) cycle intermediates and sustain amino acid biosynthesis during N assimilation (Kai et al., 2003; Masumoto et al., 2010; Lian et al., 2021). This anaplerotic role of PEPC is particularly important in roots where continuous TCA cycle replenishment is required to maintain metabolic homeostasis under varying N sources (Chen et al., 2004; Masumoto et al., 2010; Shi et al., 2015). Moreover, PEPC contributes to malate production, which is essential for pH regulation and ammonium detoxification, linking it directly to ammonium tolerance and metabolism (Koga and Ikeda, 1997; Pasqualini et al., 2001; Prinsi and Espen, 2018). Shi et al. (2015) further demonstrated that the *PPC3* isoform, which is highly expressed in roots, plays a significant role in these processes, supporting root growth and nutrient allocation under fluctuating N conditions. It has also been shown that this gene plays a key role in malate production in root nodules and could thus be responsible for N metabolism via malate synthesis in the Arabidopsis root (Chen et al., 2004). Despite these findings, the association between PEPC activity and specific root architectural traits remains largely unexplored, particularly under variable N availability.

Hormonal interactions also govern root development under varying environmental conditions. Auxin acts as a central integrator linking developmental and environmental cues and regulates root system architecture (RSA) under nitrate and ammonium nutrition (Mazzoni-Putman et al., 2021; Du and Scheres, 2018; Tognetti et al., 2012). Crosstalk between auxin and brassinosteroids (*BRs*) has been reported to fine-tune root growth responses, including primary root elongation and lateral root initiation, under distinct N regimes (Du and Scheres, 2018; Tognetti et al., 2012).

Among the molecular regulators influencing hormone signaling, Atypical Aspartic Proteases (*APs*) have emerged as intriguing, multifunctional proteins. Unlike classical *APs* that function primarily in protein degradation, atypical *APs* have been implicated in developmental and stress-response pathways (Prasad et al., 2010; Simões and Faro, 2004; van der Hoorn, 2008). It has been demonstrated that Atypical Aspartic Protease in Roots 1 (*ASPR1*) plays a significant role in root development in Arabidopsis and maize by modulating auxin balance. The overexpression of *ASPR1* disrupts auxin balance and negatively affects root growth, leading to shorter primary roots and reduced lateral root formation (Liu et al., 2023; Soares et al., 2019). Several studies suggested that atypical *APs* have specialized roles in plant physiology, indicating potential targets for enhancing root development under nutrient stress (Prasad et al., 2010; Simões and Faro, 2004; van der Hoorn, 2008). Atypical Aspartic Proteases may have broader functions in root development, potentially acting as key regulators involved in mediating hormonal crosstalk, particularly their interaction with auxin-BR signaling pathways to regulate root development under different N forms. Nevertheless, only a limited number of studies have demonstrated the atypical role of *APs* in plant root development, and further research is necessary to examine its function in plant root traits. To uncover the molecular coordination underlying these complex interactions, systems-level transcriptomic approaches such as Weighted Gene Co-expression Network Analysis (WGCNA) have become powerful tools for identifying gene modules associated with various traits (Langfelder and Horvath, 2008).

While previous studies have investigated the physiological and architectural responses of roots to N application in various plant species, few have provided an integrated analysis of dose-dependent effects of multiple N forms, anatomical traits, and transcriptomic analysis. The combination of rapid, non-invasive phenotyping and transcriptome analyses offers a promising opportunity to advance our understanding of nutrient uptake physiology and genetics. By correlating expression networks with phenotypic parameters such as root architecture, N assimilation, or enzyme activity, systems-level analysis like WGCNA enables the identification of hub genes and regulatory modules that control root adaptation to N availability. It has the potential to accelerate the identification of genes controlling N uptake and root architecture in the model species like *Brachypodium distachyon*. The objectives of this study were (1) to determine the dose-dependent effects of ammonium and nitrate on root architectural and anatomical traits, (2) to identify genes associated with general phenotypic responses to N availability using RNA sequencing (RNA-seq), and (3) to reveal co-expression modules through WGCNA that link N-dependent metabolic costs with specific anatomical and morphological traits.

Materials and methods

Growth conditions and treatments

Brachypodium distachyon is an ideal system for researching the impacts of nutrients in controlled environments due to its adaptability to various substrates like soil or sand, and its small size (Kellogg, 2015). We used Brachypodium inbred *Bd21-3* as model to study root phenotypic plasticity and focused on seedlings to detect early N adaptive responses, rather than damage caused by prolonged stress. Brachypodium seeds were sterilized for 5 minutes in 6% NaOCl + 0.1% Triton-X-100 under a clean bench and then washed five times with distilled, autoclaved water. The sterilized seeds were stored at 4°C on modified 1/3 Hogland medium containing nitrate as the N source for three days until germination at 18°C/16°C Day/night temperature in the dark. Two seedlings were then transferred to 250 ml plates with ammonium and nitrate applied as solo N form in modified 1/3 Hogland medium. The seedlings grew for up to 16 days using the grow screen agar system with 14 hours of light and 10 hours of dark. The experiment was conducted using a fully randomized block design with four repetitions and 0, 0.18 mM, 0.37 mM, 0.75 mM, 1.5 mM, 3 mM, and 6 mM N concentrations. One repetition was used for the root phenotyping and root hair microscopy. The other repetitions were used for destructive measurements, such as N content, fresh weight (FW), and dry weight (DW) measurements. The experiment was repeated four times (each with four replicates as mentioned before) using an identical experimental setup so that in total four replicates were available for root phenotyping and twelve for the destructive measurements and root hair microscopy. Missing values due to plant contamination and or poor germination, in individual replicates were excluded and replaced from other identical replicates of the same treatment from other repetitions.

In agricultural soils, available inorganic nitrogen typically fluctuates between 0.1 and 5 mM depending on fertilization regime, microbial activity, and soil moisture, with localized rhizosphere hotspots occasionally exceeding 5 mM immediately after fertilization (Giordano et al., 2021; Rubio-Asensio et al., 2014; Kabala et al., 2017; Zotarelli et al., 2007). Concentrations below 1 mM simulate low-N conditions where high-affinity transport systems dominate uptake, whereas concentrations above 3 mM reflect nutrient-rich environments that activate low-affinity transport systems (Miller et al., 2007; Noguero and Lacombe, 2016; Vidmar et al., 2000). Thus, the selected range captures both physiological extremes relevant to root nutrient foraging and transporter dynamics. To prepare media with different nitrate and ammonium concentrations, the standard one-third Hoagland formulation was modified as follows. The base medium contained KNO_3, $Ca(NO_3)_2{\cdot}4H_2O$, $MgSO_4{\cdot}7H_2O$, KH_2PO_4, micronutrients ($MnCl_2{\cdot}4H_2O$, $CuSO_4{\cdot}5H_2O$, $ZnSO_4{\cdot}7H_2O$, H_3BO_3, $Na_2MoO_4{\cdot}2H_2O$), and Fe^{3+}-EDTA. For nitrate treatments, $Ca(NO_3)_2{\cdot}4H_2O$ removed from the base medium and KNO_3 were used as the sole N sources. For ammonium treatments, nitrate salts were completely replaced with $(NH_4)_2{\cdot}SO_4$ at equimolar N concentrations. To compensate for the absence of potassium and calcium from the modified medium, we added K_2SO_4 and $CaCl_2$ to the modified 1/3 Hogland medium in the corresponding concentrations. The pH of all media was initially adjusted to 5.8 ± 0.1 before autoclaving. However, in ammonium treatments, pH tended to decrease rapidly during early seedling growth due to

ammonium uptake and proton release, which can cause root growth inhibition and toxicity. To minimize this effect, the initial pH for ammonium-containing media was adjusted slightly higher (around 6.3-6.5). In a separate experiment, we tested the impact of different pH levels on root architecture and found no significant differences (data not shown).

Our grow screen agar system was equipped with three high-throughput cameras that are able to take photos from the shoot front, above, and the root system separately (Supplementary 1). The Brachypodium seedlings were phenotyped every second day. The raw output of the phenotyping system was prepared using Photoshop and then analyzed using the RhizoVision Explorer software.

Measurement of N concentration

To determine the N concentration in Brachypodium seedlings, we harvested the 16-day old seedlings after germination and recorded their shoot and root FW. After drying the shoot and root at 60 °C for three days, we measured their DW. To analyze the N concentrations, we carefully ground the entire seedling, including the shoot and root, to a fine powder using a bead mill. We aliquoted 2 mg of this fine powder for analysis using a C/N macro elemental analyzer. By dividing the N concentration by the DW of the seedling, the total N content was calculated.

Root anatomical analysis

For our root anatomical analysis, we repeated the experiment under identical conditions and divided the root system into three equal sections corresponding to the top, middle, and bottom of the root system. We collected fresh root tissue from each section and preserved them in 75% ethanol for anatomical processing. To prepare the roots for sectioning, we solidified them in agarose and resized the blocks before gluing them onto a vibratome plate. We then used an Hm650v vibratome (Thermo Scientific Microm) to cut sections that were 40 µm thick. We collected three technical replicates for each section.

After collecting the individual sections with a fine brush, we transferred them to slides, humidified them with 1X phosphate-buffered saline, and observed them directly using a confocal microscope (Nikon C2+) to acquire images of all the sections. We then analyzed the images using custom macros that we created with the open-source "PHIV Rootcell" toolset in ImageJ (Lartaud et al., 2015). The macros allowed us to trace the outlines of the cortex, stele, aerenchyma, vessels, and cells, and count the cell files. This careful quantification enabled us to determine the sizes of the cells and vessels.

RNA extraction and transcriptome analysis

Brachypodium seeds were germinated on modified 1/3 Hogland medium with 1.5 mM nitrate for 4 days before being transferred to square petri dishes and grown for an additional 5 days. To obtain the transcriptome, nine Brachypodium seedlings were grown in a modified 1/3 Hogland medium in square petri dishes in each of three replicates. Holes were made in the petri dishes to allow the shoots to grow outside. The roots of nine plants in each replicate were harvested, pooled together, and immediately frozen in liquid N.

The frozen root tissue was ground into a fine powder using a homogenizer in liquid N. Next, 450 µL of RTL buffer containing 10 µL of beta-mercaptoethanol was added to the tube, and the tissue was homogenized using a tissue homogenizer for 5 minutes. The samples were then transferred to a RNeasy Mini spin column placed in a 2 mL collection tube and centrifuged at 10,000 x g for 10 seconds. The filtrate was transferred to a new RNase-free tube, and 202 µL of absolute ethanol was added.

The extracted RNA was sequenced using Illumina technology, and sequencing libraries were prepared with the Ion Total RNA-Seq Kit v2 following the protocol from Life Technologies, USA. Quality assessment of the sequencing data was performed using FAST-QC. Cleaned reads were then mapped to the reference genome of *B. distachyon* (Brachypodium_distachyon_v3.0_genomic) using HISAT2 software (Schaarschmidt et al., 2020). Subsequently, the data were filtered using HTseq software to count how many aligned reads overlap with the exons of each gene. To account for library size and compositional differences, normalization was performed using the Trimmed Mean of M-values (TMM) method implemented in the edgeR package. Prior to differential expression gene analysis (DEG), low-abundance genes were filtered out based on counts per million (CPM) thresholds (genes with zero reads across all samples were removed). To correct for potential batch effects in the RNA-Seq data, we applied the ComBat_seq function from the sva R package. The edgeR package also was utilized to identify DEGs, with a significance threshold of P value < 0.05 and a false discovery rate threshold of FDR < 0.1. Using a General Linear Model (GLM), we compared low versus moderate, low versus high, and moderate versus high concentrations of nitrate and ammonium. Gene ontology (GO) for biological processes were performed for DEGs using the "enricher" function of the "Biomart" library (Durinck et al., 2009) and visualized using clusterProfiler package in R (Yu et al., 2012).

Weighted gene co-expression network analysis

Normalized RNA-seq data were analyzed using the WGCNA package in R to explore correlations between the transcriptome and the physiological phenotypes across the various treatments (Langfelder and Horvath, 2008). Genes with zero values in all samples were excluded from the dataset and the remaining genes were used in the construction of weighted gene co-expression networks. Pearson correlation matrices for gene expression were computed for each network and transformed into connection strength matrices using an appropriate power function (soft-thresholding power $\beta = 8$) to ensure scale-free behavior. These

connection strengths were then converted into a Topological Overlap Matrix (TOM).

TOM combined with average linkage hierarchical clustering was applied via the DynamicTree Cut algorithm to identify distinct co-expressed genes modules. To link these modules to phenotypic data, expression data was integrated with phenotypic responses across all N treatments. Modules with a correlation coefficient ≥ 0.4 and a p-value ≤0.05 were considered significant and selected for further analyses. Within each significant module, module membership and gene significance were calculated for all genes and the top genes were then identified based on their module membership and gene significance for the phenotype of interest and were further investigated.

Phenotypic data analyses

Phenotypic data were analyzed with R (R Core Team, 2013). Mean trait values were computed for each treatment, and the variation among the mean trait values of the two N treatments and concentrations was evaluated using analysis of variance (ANOVA). When the ANOVA indicated significance at the 5% probability level, the Tukey's HSDtest was used to assess differences between treatments.

Results

Phenotypic analysis

Ammonium and nitrate treatments affect biomass allocation and N uptake

Whole plants were harvested to measure N content, as well as FW and DW. The total DW increased as N concentration increased; however, ammonium treated plants showed significantly greater biomass (P value $=2.14\times10^{-3}$) than those receiving nitrate (Figure 1A). This increase in total DW was primarily due to increased shoot biomass, while root biomass decreased with increasing N concentration (Figure 1A). At lower N concentrations, around 65% of total biomass was allocated to the roots, while this allocation dropped to approximately 30% at higher N concentrations. The observed difference in total DW at 0 mM nitrate and ammonium likely reflects baseline physiological variation arising from minor pH differences during media preparation and natural seed heterogeneity rather than N treatment effect (data not shown). Across all N concentrations, plants grown with ammonium generally took up more N per milligram DW than those grown with nitrate (Figure 1B), which likely contributed to the greater overall biomass of ammonium treated plants; a difference that became more evident in the higher range of N concentrations. The N content in plant tissues increased up to a concentration of 1.5 mM for both N forms and remained constant from 1.5 to 6 mM. However, nitrate treated plants absorbed more N per unit of root length, primarily because they achieved this uptake with a shorter total root length (Supplementary 1).

RSA has differential responses to N forms and concentrations

Similar to root DW, total root length decreased with increasing N concentrations, where root architecture adapted to both N forms and concentrations (Figure 1E). Reduced total root length in response to increasing N concentration was accompanied by decreases in root system area and root volume (Supplementary 1). However, compared to nitrate-grown plants, ammonium-grown plants exhibited greater total root length, network area, root volume, and surface area with less variation in root phenotype across different total N concentrations. In contrast, plants grown with nitrate exhibited two distinct response plateaus, one at low N concentrations, corresponding to the range of high-affinity nitrate transporters (HATS) (0 to 0.37 mM), and another at higher concentrations, associated with low-affinity nitrate transporters (LATS) (0.75 mM to 6 mM) (Khramov et al., 2024; Orsel et al., 2007) (Figure 1D). Across all treatments, each plant produced only one seminal root, which was longest under low N conditions, with its length decreasing as N concentrations increased. This decline was particularly pronounced with nitrate application. Longer seminal roots produced more lateral branches (Supplementary 1), although branching frequency remained relatively constant across different N concentrations and sources (Supplementary 1).

N forms and concentrations shape root hair development and lateral root architecture

Plants treated with ammonium developed a more extensive root area primarily due to an increase in the number of branched roots. Although low nitrate concentrations also stimulated more root branching, the average length of lateral roots remained relatively stable across the different N concentrations and forms (Figure 1C). However, at lower nitrate concentrations (0.1875 mM and 0.375 mM), plants developed significantly longer lateral roots than at high nitrate concentrations. In contrast, at higher N concentrations (1.5 mM, 3 mM, and 6 mM), ammonium treated plants exhibited a significantly greater total lateral root length compared to those grown in nitrate (Pvalue= 7.28×10^{-9}). Additionally, ammonium treated plants produced more secondary-order lateral roots, whereas increasing nitrate concentrations induced the formation of root hairs (Figure 2A). Microscopic examination revealed that the formation of root hairs on seminal roots was significantly (Pvalue= 2×10^{-16}) affected by both the form and concentration of N. Plants exposed to ammonium had reduced root hair density and length compared to those treated with nitrate (Figure 2B). Interestingly, a slight but consistent increase in both root hair length and density was observed at low ammonium concentrations (0.18 mM and 0.37 mM). This transient stimulatory effect may reflect a localized adaptive response of root epidermal cells to mild ammonium availability. Low external ammonium can momentarily enhance proton fluxes and activate auxin transport, thereby stimulating epidermal cell expansion and root hair initiation (Lima et al., 2010; Meier et al., 2020). However, at higher ammonium levels, excessive proton release and cytosolic acidification likely inhibit cell elongation and suppress root hair growth, consistent with ammonium-induced toxicity reported in previous studies (Britto and Kronzucker, 2002; Liu

10.3389/fpls.2025.1708928

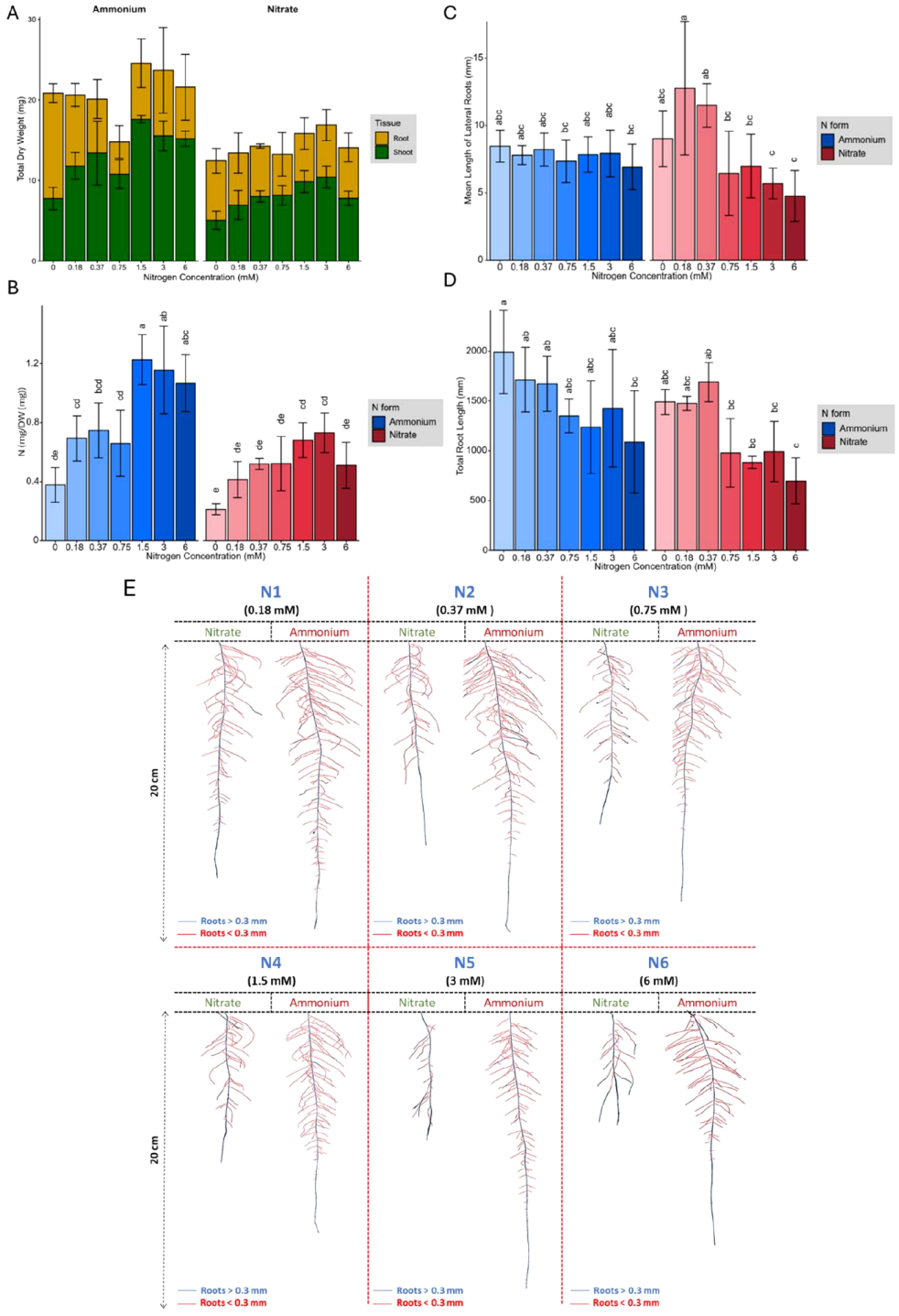

FIGURE 1
(A) Root and shoot dry biomass, **(B)** Nitrogen content per gram of total dry biomass, **(C)** Mean length of lateral roots (mm), **(D)** Total root length (mm), in response to 0 mM, 0.18 mM, 0.37 mM, 0.75 mM, 1.5 mM, 3 mM, and 6 mM ammonium and nitrate concentrations in the growth media. **(E)** Response of Brachypodium distachyon root system architecture of plants grown under various nitrate and ammonium concentrations. The red color represents roots with a diameter of less than 0.3 mm (lateral roots), while the blue color represents roots with a diameter of more than 0.3 mm (seminal root). Representative plants for each condition are shown. In **(B)**, **(C)**, and **(D)**, error bars represent the standard error of the mean, and letters indicate statistical significance between groups ($p < 0.05$).

10.3389/fpls.2025.1708928

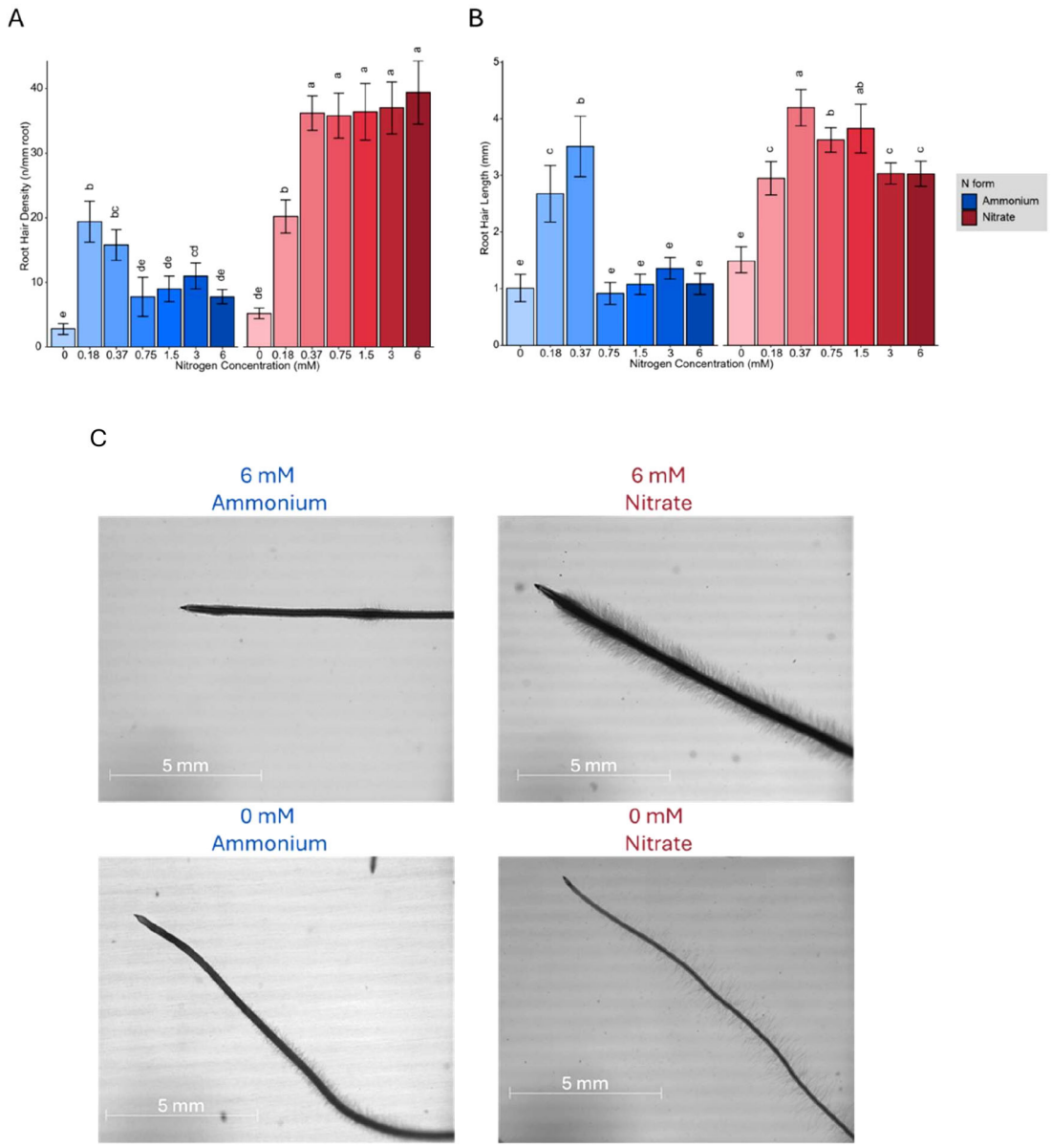

FIGURE 2
(A) Root hair density (hairs per mm root) and **(B)** Root hair length (mm) of Brachypodium distachyon plants grown under different nitrogen concentrations (0, 0.18, 0.37, 0.75, 1.5, 3, and 6 mM) of ammonium (blue) and nitrate (red). **(C)** Representative images of Brachypodium root hair morphology at 6 mM and 0 mM of ammonium (left) and nitrate (right). Scale bars represent 5 mm. In **(A)** and **(B)**, error bars represent the standard error of the mean, and letters indicate statistical significance between groups ($p < 0.05$).

and von Wirén, 2017). In contrast, plants treated with nitrate showed distinct responses depending on the concentration. At low nitrate concentrations, root hairs were longer, but had significantly lower density compared to those at higher nitrate concentrations (Pvalue= 2×10^{-16}), where root hair density increased despite a reduction in their length (Figure 2C).

Root aerenchyma formation and anatomical features have distinct differences in response to ammonium and nitrate

We also examined the effects of varying N concentrations on root anatomy by dividing the seminal roots into three sections (root base, middle, and tip) of equal-length and taking cross-sections of each (Supplementary 1). The anatomy of the roots varied significantly (Pvalue= 5.47×10^{-4}) across these sections (Figure 3E). The root cross-sectional area increased with rising nitrate concentrations. At high nitrate concentrations, the root cross-sectional area was larger in the younger root sections compared to the basal sections (Figure 3A). In contrast, ammonium application significantly (Pvalue= 2.66×10^{-11}) reduced the cross-sectional area, with younger root sections being smaller (Figure 3A). Thicker roots with greater cross-sectional areas generally exhibited an expanded cortical area without a corresponding increase in stele area (Figure 3B). This expansion

10.3389/fpls.2025.1708928

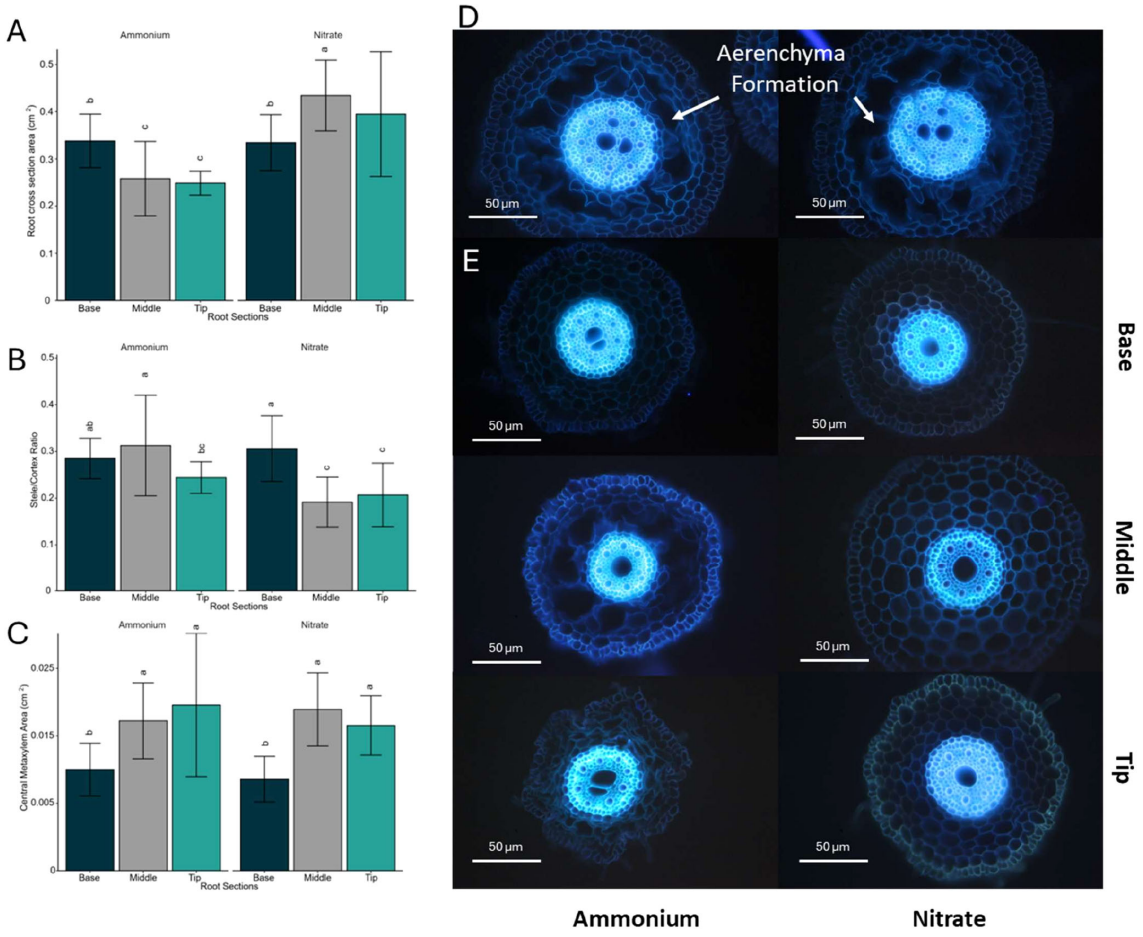

FIGURE 3
Root anatomical characteristics assessed in their response to ammonium and nitrate. **(A)** Root cross-sectional area (cm^2), **(B)** Stele/cortex ratio, **(C)** Central meta xylem area (cm^2) in three regions of the root (Base, Middle, Tip) (dark green /gray /green) under ammonium (left) and nitrate (right) treatments. **(D, E)** Fluorescence microscopy images of root cross-sections show structural differences between ammonium (left) and nitrate (right) treatments. The sections are arranged by root region (Base, Middle, Tip). In **(A–C)** error bars represent standard error of mean, and letters indicate statistical significance between groups ($p < 0.05$).

of the cortical area was primarily due to an increase in cell size rather than cell number (Supplementary 1). Although the stele area remained relatively unchanged (Supplementary 1), the central metaxylem area measured as fraction of the total stele area, significantly increased (Pvalue= 2.27×10^{-7}) from the root base to the middle and tip in both ammonium and nitrate treatments across all concentrations (Figure 3C). Ammonium treated roots were generally thinner than nitrate treated roots, primarily due to a reduced cortex area (Figure 3E). Higher ammonium concentrations not only decreased cortical thickness but also induced the formation of aerenchyma in the upper (older) sections of the roots (Figure 3D). Plants exposed to high ammonium concentrations showed a reduced living cortical area, caused by narrower cortical cells and fewer living cortical cell files. In contrast, basal root sections remained largely unaffected, with no significant differences detected across N concentrations or forms.

Transcriptional analysis

Differentially expressed genes in response to N form and concentration

Using a GLM analysis across all comparisons of N concentrations, we identified 5,517 genes that were significantly differentially expressed under ammonium application, and 2,538 genes that were significantly expressed in response to nitrate applications (Supplementary 1). For both N forms, we used the lowest N concentration as the reference and compared all other N concentrations against it. Most of these genes were differentially abundant between high and low N concentrations, with few significant differences observed between low and moderate or moderate and high concentrations (Supplementary 1). The clustering patterns observed in the Principal Component Analysis (PCA) of transcript levels closely mirrored those from RSA

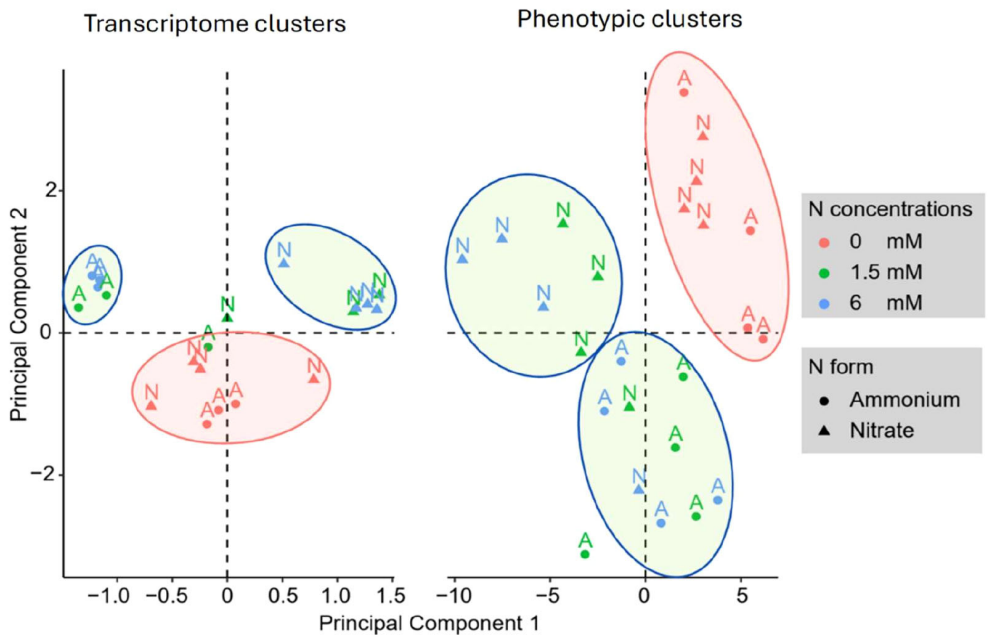

FIGURE 4
Principal component analysis of *Brachypodium distachyon* gene expression (left) and phenotypic traits (right). The scatter plots illustrate the clustering of differentially expressed genes (DGE clusters) and phenotypic traits (Phenotypic clusters) under varying nitrogen levels (0, 1.5, and 6 mM) and nitrogen sources (ammonium and nitrate). Color coding reflects nitrogen concentrations (red for 0 mM, green for 1.5 mM, and blue for 6 mM), while the shape represents nitrogen form. Clusters are visually separated by ellipses to indicate groupings of similar responses.

measurements, which were based on 29 distinct traits (Figure 4). The PCA consistently grouped samples from the same treatment together, indicating a strong alignment between gene expression profiles and root system characteristics (Figure 4).

To visualize the biological processes affected by N treatment, the gene ontology of significantly expressed genes were found using the "enricher" function of the "Biomart" library in R (Durinck et al., 2009). Gene ontology (GO 2.62.0) enrichment analysis revealed distinct patterns in gene regulation in response to N application. In nitrate treated plants, genes involved in the response to other nutrients (such as phosphate, cadmium, and sulfate) were upregulated in both high and moderate nitrate conditions compared to low nitrate conditions. Conversely, gene families associated with N transport were downregulated at moderate nitrate concentrations compared to low nitrate concentrations (Supplementary 1). In ammonium treated plants, high ammonium concentrations led to upregulation of genes related to cytokinin activity and chloroplast functions. However, genes associated with auxin activity, carbohydrate transport, and water channels were downregulated at both high and moderate ammonium concentrations compared to low ammonium concentrations. Notably, genes involved in anatomical development and cellulose activity were also downregulated at high ammonium concentrations suggesting their close relationship with ammonium uptake and metabolism (Supplementary 1).

High and low affinity nitrate transporter and ammonium transporter activities respond to N applications

Overall, the gene expression/transcript levels of nitrate and ammonium transporters was more sensitive to N concentration than to N form. We analyzed five genes that were previously identified as low-affinity nitrate transporters, individually (Supplementary 1) (Guo et al., 2014; Sigalas et al., 2024). The DEG analysis revealed that the *NRT1.1* gene, a low-affinity nitrate transporter, was upregulated in response to higher nitrate applications (Figure 5). However, *NRT1.2* and *NRT1.3* did not show significant (Supplementary Data 1) changes across nitrate concentrations (Figure 5). Conversely, *NRT1.4* and *NRT1.5* were upregulated at moderate nitrate concentrations (Figure 5) compared to low nitrate concentrations. Among high-affinity nitrate transporters, seven out of nine members were expressed in both ammonium and nitrate application, with five belonging to the *NRT2* family and two to the *NRT3* family. The *NRT3* gene family showed consistent expression across all nitrate concentrations (Figure 5). In contrast, *NRT2*.1, *NRT2*.2, and *NRT2*.4 were upregulated with increasing nitrate concentrations, while *NRT2*.5 and *NRT2.7* were dramatically (Supplementary Data 1) downregulated at high nitrate concentrations (Figure 5). Additionally, at high ammonium concentrations, the gene families responsible for ammonium transporters (*BRADI_1g02420v3* and *BRADI_3g45480v3*) were downregulated by approximately two-fold (Figure 5).

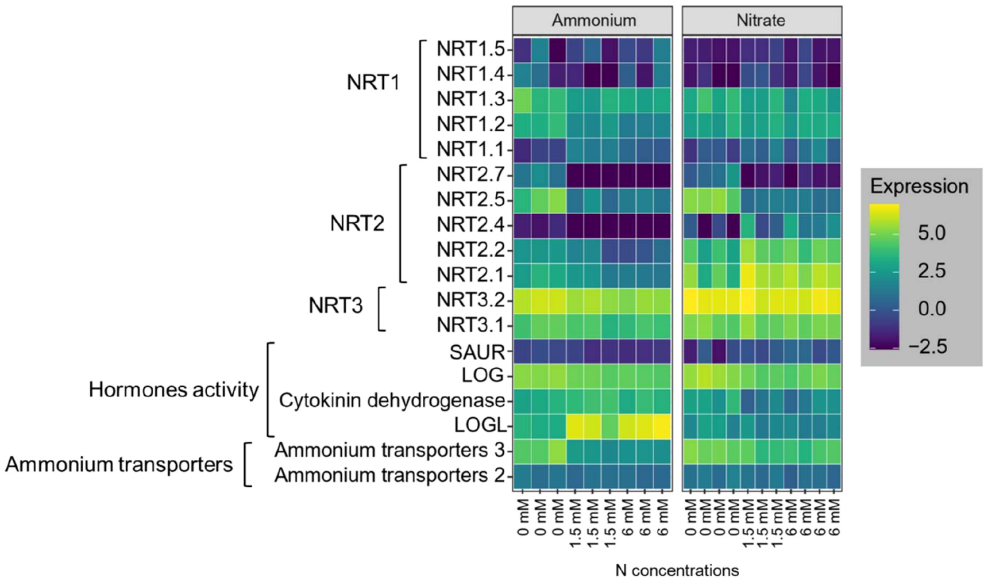

FIGURE 5
Heatmap of gene expression levels related to nitrate transporters (NRT1, NRT2, and NRT3), hormones activity, and ammonium transporters in Brachypodium roots under ammonium and nitrate treatments at varying nitrogen concentrations (0, 1.5, and 6 mM). The experiment had three replicates.

Contrasting gene expression was observed for genes coding for phytohormone in response to ammonium and nitrate

Gene ontology enrichment analysis revealed significant changes in the expression of phytohormone coding genes in plants grown with ammonium compared with those in nitrate. Specifically, genes associated with cytokinin, and auxin pathways were notably affected. In ammonium-treated plants, a downregulation of genes involved in auxin signaling, including the *SAUR* family gene *BRADI_3g05020v3* (Figure 5) was observed. Conversely, the cytokinin-related gene *LOGL* (*BRADI_3g28900v3*) was significantly upregulated in ammonium-treated roots (Pvalue= 1.66×10^{-6} for low ammonium vs moderate ammonium, Pvalue= 1.75×10^{-7} for low ammonium vs high ammonium), suggesting its role in promoting lateral root growth and development (Figure 5). However, some other cytokinin signaling genes, including *LOG* (*BRADI_2g42190v3*) and Cytokinin dehydrogenase (*BRADI_2g05580v3*), were downregulated in response to both ammonium and nitrate applications regardless of their concentration (Figure 5). This targeted analysis of hormonal response genes helps clarify the molecular mechanisms by which different N forms modulate root development, as indicated in prior studies (Asim et al., 2020; Dziewit et al., 2024; Kazan, 2013; Naulin et al., 2019).

Aquaporin related genes and water channel activity in ammonium application

Given the crucial role of aquaporins in regulating water and N transport within plant roots, analyzing specific aquaporin gene responses under varying N sources can help elucidate their roles in managing nutrient uptake and preventing N toxicity (Wang et al., 2016). The aquaporin gene family members *TIP4-2* (*BRADI_2g07830v3*), *TIP2-1* (*BRADI_2g62520v3*), *TIP5-1* (*BRADI_5g17680v3*), and *TIP4-3* (*BRADI_2g07810v3*) were downregulated in plant roots grown under elevated ammonium concentrations (Supplementary 1). Conversely, in roots grown under nitrate conditions, these genes (except *TIP4-2*) were upregulated as the N concentration increased. The downregulation of *TIP4–2* in response to higher ammonium concentrations aligns with the downregulation of ammonium transporters, suggesting a similar role in preventing N excessive accumulation, particularly as total N uptake per unit root length becomes saturated at 1.5 mM external N (Figure 1B).

Correlation of gene modules with root traits highlights distinct N uptake strategies

To uncover key genes contributing to the observed root phenotypes upon N treatment, WGCNA was performed across ammonium and nitrate treatments. This approach identified 32 co-expressed gene modules which were in the following designated according to the assigned color (Figure 6). Each module contained from 45 to 2,923 genes. We tested the correlation of each module's eigengene with the root morphological and anatomical phenotypes as well as N content of the plants. Correlation analysis of module eigengenes with phenotypic traits revealed several significant associations (Figure 7).

Two modules, "light green" (including 350 genes) and "dark red" (including 205 genes), exhibited striking contrasts with root traits (Supplementary Data 4). The "light green" module was positively correlated with traits related to root elongation (total root length ($|r| = 0.83$) and mean lateral root length ($|r| = 0.71$)), and negatively correlated with root hair traits and anatomical features

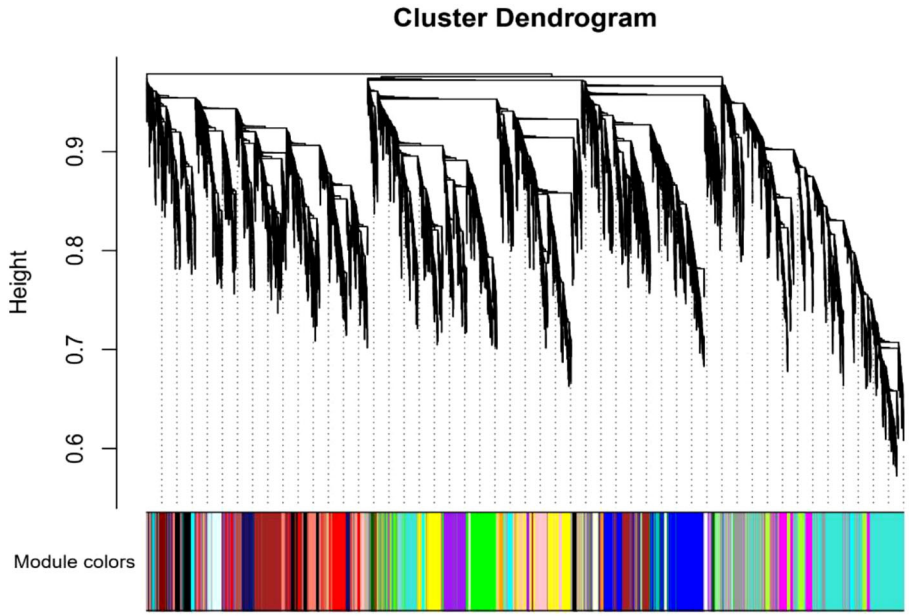

FIGURE 6
The dendrogram shows the hierarchical clustering of genes into modules based on their co-expression patterns. Each module is represented by a different colored bar below the dendrogram. Modules group genes that are highly co-expressed, indicating similar functional or regulatory roles in response to nitrogen treatments.

(Figure 7). In contrast, the "dark red" module was associated with more compact root systems, but it showed positive correlations with root hair development (root hair length |r| = 0.33 and density |r| = 0.96) (Figure 7). These contrasting gene-to-trait associations between the two modules suggests different strategies of root adaptation to N availability, either elongation to explore more soil volume ("light green") or increasing surface area through root hairs ("dark red"). The "yellow" (including 1619 genes) and "brown" (including 1770 genes) modules also displayed contrasting relationships with respect to N content (Supplementary Data 4). The "yellow" module was positively correlated with total N content (|r| = 0.79), while the "brown" module was strongly negatively correlated with N content (|r| = 0.78), suggesting different roles for the genes within these modules toward N uptake or storage efficiency (Figure 7).

Intramodular analysis identifies key genes correlated with root phenotypes

For each module, genes with high Gene Significance (0.9 < GS) and Module Membership (0.8<MM) scores were examined to identify genes that may contribute to the underlying mechanisms governing root development in response to N application. We identified key genes within the modules that showed significant correlations with various root phenotypes. Through ontology enrichment of these genes, and their homologues in rice, Arabidopsis, and maize, we elucidated their function using the gProfiler (Raudvere et al., 2019) and NCBI database for annotation, visualization, and integrated discovery (DAVID) tool (Huang et al., 2007). Among these identified key genes, we selected genes with top rank and significant expression for further analysis (Table 1).

Following these criteria, investigation of the light green module identified the potential hub genes *BRADI_1g42930v3*, a homolog of an aspartyl protease family protein (*APs*, *At5g10770*), *BRADI_1g35100v3* (*SAUR32*), a gene encoding an auxin-responsive protein, *BRADI_2g38330v3*, which is involved in zinc ion transmembrane transport, and *BRADI_4g13960v3*, a gene associated with root-specific metal transporter responses. These genes had similar expression patterns under low N conditions but were downregulated under high N conditions, with more pronounced suppression in the presence of nitrate than ammonium (Figure 7).

Investigation of the dark red module identified the hub genes *BRADI_1g12280v3*, a homolog of HPP in maize and Arabidopsis, *BRADI_1g39167v3* (phosphoenolpyruvate carboxylase 1, PEPC1), *BRADI_1g14780v3* (LOB domain-containing protein 37), and *BRADI_1g73970v3* (SULFUR DEFICIENCY-INDUCED 2) among others (Table 1, Figure 7). Genes in the dark red module were upregulated under moderate and high nitrate conditions but suppressed under low nitrate conditions and across ammonium treatments (Figure 7). Positive module-trait correlations were observed for cortex, stele, and root cross-sectional areas and root hair density, while there was a strong negative correlation with total root length.

The yellow module contained the genes *BRADI_2g12580v3* (cysteine-rich receptor-like protein kinase 15) and *BRADI_3g55120v3* (PHOSPHATE STARVATION RESPONSE 2), which were positively correlated with N content in the whole plant and were highly expressed in the presence of higher N concentrations under both ammonium and nitrate applications (Figure 7). Both genes responded more strongly to nitrate application (downregulated in comparison with ammonium

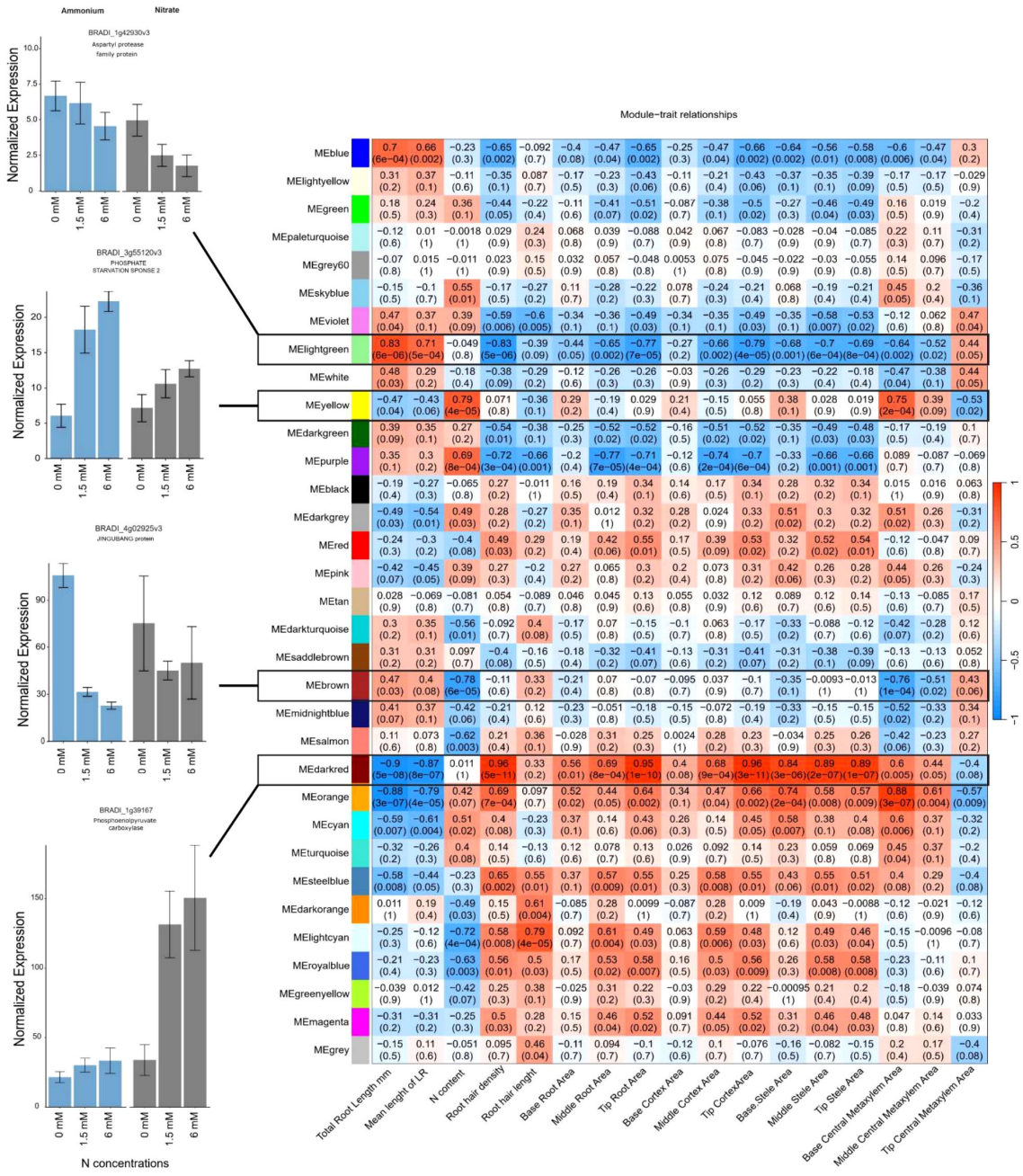

FIGURE 7
The heatmap (right) depicts the correlation between gene expression modules and root traits of interest across nitrogen treatments. Each cell represents the Pearson correlation coefficient between a module's eigengene (the first principal component of gene expression within a module) and a specific trait, with corresponding p-values in parentheses. Positive correlations are shown in red and negative correlations are shown in blue. Bar plots (left) are representative of each module normalized gene expression in *Brachypodium distachyon* in response to nitrogen-free, 1.5 mM, and 6 mM ammonium (left) and nitrate (right) conditions. Error bars represent the standard error of the mean, with normalization performed using the TMM method.

application), however, *BRADI_2g12580v3* was significantly suppressed under low N conditions (Supplementary Data 2). Conversely, the brown module contained *BRADI_1g67440v3* (FAF-like, chloroplastic) and *BRADI_4g02925v3* (protein JINGUBANG), which were negatively correlated with N content where their expression was suppressed under high N concentrations, and this effect was exacerbated in response to ammonium compared to nitrate (Figure 7).

Discussion

Strong associations between root phenotypes and transcriptomic responses suggest distinct transcriptional programs across traits

Root architecture and anatomical traits, which are presumably controlled by many genes, exhibit significant phenotypic plasticity

10.3389/fpls.2025.1708928

TABLE 1 Genes identified with high gene significance and module membership scores in each module for root phenotypes in response to N application.

Gene ID	Gene name	Module	Positive correlation	Negative correlation
BRADI_1g67440v3	Protein FAF-like, chloroplastic	Brown		Nitrogen content
BRADI_4g02925v3	Protein JINGUBANG	Brown		Nitrogen content
BRADI_1g14780v3	LOB domain-containing protein 37	Dark red	Root hair density	Total root length
BRADI_3g53601v3	Uncharacterized LOC104581291	Dark red	Root hair density	Total root length and mean of lateral root
BRADI_1g73970v3	Protein SULFUR DEFICIENCY-INDUCED 2	Dark red	Cross-sectional area	
BRADI_1g39167v3	Phosphoenolpyruvate carboxylase 1	Dark red	Cortex, stele, and root cross-sectional area, root hair density	Total root length
BRADI_1g12280v3	Uncharacterized LOC104582693	Dark red	Root hair density, cortex, stele, and root cross-sectional area	Total root length
BRADI_2g05640v3	Clavaminate synthase-like protein At3g21360	Dark red	Cross-sectional and cortex area	
BRADI_4g24950v3	Proline-rich protein haeiii subfamily 1	Dark red	Root cross-sectional and cortex area	
BRADI_3g54507v3	Uncharacterized	Dark red	Root cross-sectional and cortex area	
BRADI_2g38330v3	Involved in zinc ion transmembrane transport	light-green	Mean length of lateral roots and total root length	
BRADI_4g13960v3	Root-specific metal transporter	light-green	Total root length	
BRADI_1g42930v3	Aspartyl protease family protein At5g10770	light-green	Mean length of lateral roots and total root length	Root hair density, cortex and root cross-sectional area, stele area
BRADI_4g44427v3	Probable serine/threonine- protein kinase WNK8	light-green		Root cross-sectional and cortex area
BRADI_3g42290v3	Protein DETOXIFICATION 33	light-green		Cross-sectional and cortex area
BRADI_2g15720v3	3-ketoacyl-coa synthase 11	light-green		Root cross-sectional and cortex area
BRADI_2g35197v3	Serine carboxypeptidase 2	light-green		Root cross-sectional and cortex area
BRADI_1g35100v3	Auxin-responsive protein SAUR32	light-green		Cortex and root cross- sectional area, root hair density
BRADI_1g26990v3	Expansin-like B1	Orange	Central metaxylem	
BRADI_3g11430v3	Nicotianamine aminotransferase A	Orange	Central metaxylem	
BRADI_2g12580v3	Cysteine-rich receptor-like protein kinase 15	Yellow	Nitrogen content	
BRADI_3g55120v3	Protein PHOSPHATE STARVATION RESPONSE 2	Yellow	Nitrogen content	

across different environments. They can adapt and change their structure in response to varying environmental conditions (Bray and Topp, 2018). These traits are influenced by genetic and environmental factors, allowing the plant's roots to adapt and modify their structure depending on environmental conditions. Despite varying responses to N application among crop species, many of these traits have a conserved transcriptional response, suggesting a common genetic basis for adaptation to unfavorable conditions (Rogers and Benfey, 2015). We observed that root responses to ammonium and nitrate vary depending on their concentration and suggest that these responses are part of a nutrient foraging strategy to maximize root uptake area while minimizing the root system's metabolic costs and preventing excessive nutrient accumulation.

Our study identified two key genes, *BRADI_1g42930v3*, which encodes an aspartyl protease family protein (APs), and *BRADI_1g39167v3*, which encodes phosphoenolpyruvate carboxylase 1 (*PEPC1*), whose transcript levels correlated with the expression of numerous genes involved in root anatomical and morphological responses across varying concentrations of

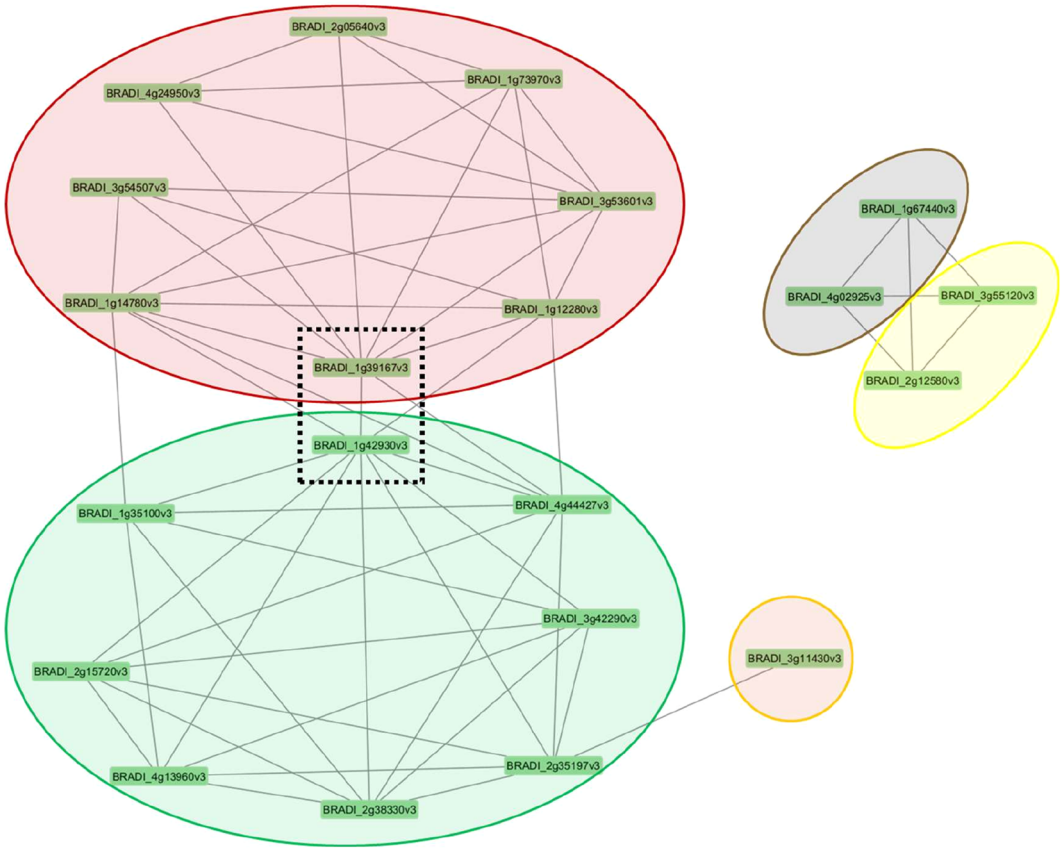

FIGURE 8
Clusters of co-regulated genes in *Brachypodium distachyon* under different nitrogen conditions. The network diagram displays modules of co-expressed genes, represented by colored ovals, with each node corresponding to an individual gene. The lines between genes indicate significant co-expression relationships calculated using topological overlap matrix. The central genes within the dashed box (BRADI_1g39167v3 and BRADI_1842930v3) appear to link the two major modules (red and green), suggesting they may play a key regulatory role in connecting these gene networks.

ammonium and nitrate (Figure 8). These two genes showed the highest betweenness centrality scores among all hub genes (Supplementary Data 3). A high degree betweenness centrality score indicates that a node has more connections with other nodes than the average (Kumar and Mukhtar, 2023). These genes potentially contribute to the optimization of metabolic costs by regulating root growth patterns that are responsive to nutrient availability. This is supported by previous functional studies which have highlighted the role of *PEPC1* in root architecture and N metabolism. Overexpression of *PEPC1* in rice demonstrated its influence on RSA, where a smaller root system formed including shorter primary roots at the seedling stage, as a response to altered metabolic fluxes (Lian et al., 2021). These changes were closely associated with adjustments in N assimilation and the expression of genes linked to the TCA cycle and glycolysis, highlighting the role of *PEPC1* in balancing nutrient uptake and metabolic energy costs. This evidence underscores the potential of *PEPC1* as a key player in optimizing root growth and nutrient use efficiency in response to environmental conditions.

On the other hand, an aspartyl protease family protein (*ASPR1*) was shown to play a critical role in lateral root formation in *Arabidopsis thaliana* (Soares et al., 2019). Loss of function mutations in *ASPR1* led to a significant reduction in lateral root density, while it's expression enhanced root branching. These findings suggest that expression of *APs* also have a role in controlling RSA to optimize nutrient uptake and minimize metabolic costs. The involvement of *APs* in processes like lateral root initiation further supports their role in nutrient foraging strategies, complementing the activities of *PEPC1* and its regulation of N uptake and metabolic efficiency.

An aspartyl protease gene strongly correlated with root architecture response to low N availability

The Brachypodium *APs* gene was strongly correlated with larger root system and lateral root development response under low N availability. Increasing the concentrations of nitrate and ammonium resulted in a smaller root system, characterized by reduced total root length and lateral root length. These traits are important for maximizing soil exploration and accessing N distributed in the soil profile (Lynch, 2019; Rogers and Benfey, 2015). Previous studies in Arabidopsis and maize have

demonstrated similar results that the root foraging response to N deficiency involves the production of a large root system by elongation of both primary and lateral roots (Gao et al., 2014; Jia et al., 2019; Tian et al., 2005). A larger root system with a greater number of lateral branches increases the spatial extent of the root system, thereby enhancing the ability to acquire N from heterogeneous soils (Guo et al., 2014). However, some studies have shown an opposite response where N deficiency reduces root system area by decreasing lateral root density in cereals, including maize and rice (Ravazzolo et al., 2019). In rice, N deficiency modulated auxin levels, producing a smaller root system due to reduced number of lateral roots (Sun et al., 2019). The contrasting results of the two latter studies compared to the previous studies and our own results are likely due to different experimental conditions and sampling stages. For instance, rice studies used a half-strength growth medium containing only ammonium as N source, while we used an N-free medium as the lowest N concentration. Additionally, after two weeks, the N concentration in the Brachypodium plants matched that of the non-germinated seeds, indicating that the plants primarily relied on their seed reserves during this early growth stage.

Auxin is a key regulator of lateral root development, influencing various stages from initiation to emergence. It promotes the formation of lateral root primordia by modulating cell division and expansion in the pericycle cells of the root (Du and Scheres, 2017). Our co-expression network analysis showed that *BRADI_1g35100v3* which encodes the auxin-responsive protein *SAUR32* was co-expressed with the *APs* gene (*BRADI_1g42930v3*) (Figure 8). We reported that the expression of auxin-responsive protein *SAUR32* (*BRADI_1g35100v3*) was negatively correlated with root cross-sectional area and root hair density (Figures 7, 2A, 3A). In Arabidopsis, it has been reported based on aspr1 mutants that this gene is involved in the deregulation of proteins associated with reactive oxygen species and auxin homeostasis, which is known to affect the number of lateral roots (Soares et al., 2019). For instance, APs protein family regulates auxin signaling by inhibiting the activity of AUXIN RESPONSIVE FACTORS (*ARFs*) during root growth (Cui et al., 2024; Rogg and Bartel, 2001; Soares et al., 2019; Su et al., 2020; Vierstra, 2009). In low N concentrations, APs gene could potentially influence lateral root development indirectly by modulating AUXIN RESPONSIVE FACTORS (*ARFs*), leading to either a reduction or an increase in lateral root growth. Under normal nutrient conditions, expression of the *BRADI_1g42930v3* homolog, *ASPR1*, in Arabidopsis led to reduced primary root growth and inhibited lateral root development (Soares et al., 2019), indicating its functional role in root formation. However, under N deficiency, no significant reduction in lateral root length was observed (Soares et al., 2019). Notably, in that study, the transcription level of *ASPR1* was not quantitatively assessed. In contrast, our results showed that *ASPR1* suppression was correlated with the application of higher N concentrations, resulting in a reduced root system size and shorter lateral roots (Figures 7, 1C). A recent genome-wide association study in maize highlighted the role of the *GRMZM2G468657* gene, another homologue of *APs* in Brachypodium (*BRADI_1g42930v3*), in root development and response to N deficiency (both its expression and polymorphisms) (Liu et al., 2023). To date, these two studies are the only ones that explored the role of the aspartic protease gene family in root architecture formation.

The Brachypodium *APs* gene was also correlated with root structural changes at the anatomical level. Under ammonium and low nitrate application, *APs* gene expression was upregulated and associated with reduced root hair density and thinner roots. Root hairs significantly enhance the absorptive surface area, playing a crucial role in capturing immobile forms of N, such as ammonium (Zhiyong et al., 2022). The cross-sectional area, including the stele, influence the storage, transport, and metabolic efficiency of N absorbed from the soil (Burton et al., 2015). Larger stele areas can enhance vascular transport capacity, thereby improving the overall efficiency of nutrient transport to aboveground plant parts (Li et al., 2023; Lynch et al., 2021; Wang et al., 2019). It is reported that *APs* are also involved in programmed cell death in Arabidopsis and rice flowers (Niu et al., 2013; Phan et al., 2011). In roots, programmed cell death plays a crucial role in aerenchyma formation (Drew et al., 2000). It could highlight the potential roles of *APs* in root aerenchyma formation in higher N concentrations by modulating the programmed cell death in the root cortex area. However, this requires further research.

These explanations illustrate that *APs* gene (*BRADI_1g42930v3*) emerges as a potential regulator of root development and N response in Brachypodium, interacting within complex biological networks involving hormone signaling and root architecture. Our results indicate its co-expression with ten other genes across different modules (Figure 8), suggesting functional relationships and coordination. Previous studies proposed that atypical aspartic proteases may have regulatory roles beyond housekeeping functions (Simões and Faro, 2004). We showed that *APs* gene (*BRADI_1g42930v3*) could potentially modulate the root hormones as it was correlated to the expression of the *BRADI_1g14780v3*, which encodes a LOB domain-containing protein 37 correlated with root hair density and *SAUR* gene (*BRADI_1g35100v3*). Additionally, *BRADI_1g14780v3*'s co-expression with uncharacterized genes *BRADI_1g12280v3* and *BRADI_3g53601v3* further supports its role in N response and root formation. Interestingly, its transcript levels were associated with a *PEPC 1* homolog (*BRADI_1g39167v3*) and exhibited contrasting correlations with various root phenotypes, highlighting its multifaceted regulatory potential.

Reduction of metabolic costs by *PEPC* in response to higher N availability

The negative correlation of *PEPC1* (*BRADI_1g39167v3*), a gene involved in carbon/nitrogen metabolism, with mean length of lateral roots and total root length suggested the adjustments at transcription scale to reduce metabolic costs associated with roots growth under N supply conditions. *PEPC1* plays an anaplerotic role in replenishing the TCA cycle intermediates and is involved in the

plant's response to stress conditions (Feria et al., 2016; Prinsi and Espen, 2018; Shi et al., 2015). The reduced expression of *PEPC1* and *APs*, along with the role of co-expressed genes such as *SAUR* and Aquaporin indicate a strategy to maintain efficient N uptake while reducing energy demands, thereby achieving a functional balance between root and shoot growth. Specifically, the downregulation of *PEPC1* and *APs* upon (Figure 7) suggests that energy-intensive processes are being minimized. Meanwhile, *SAUR* genes, which are often involved in auxin signaling, could be playing a role in adjusting root growth patterns to optimize resource allocation. Aquaporins, which facilitate water and nutrient movement, help maintain proper nutrient transport with minimal energy expenditure. Thus, these adjustments allow the plant to conserve energy by modulating root activity, ensuring that N uptake is balanced with the energy needs of both root and shoot growth, maintaining a functional balance between these two systems.

Differential regulation of *PEPC1* under ammonium and nitrate

When N is abundant in the environment, especially in the form of NO_3^-, we observed smaller root systems and increased shoot biomass. Unlike previous long-term hydroponic studies, our short-term agar experiment revealed increased shoot biomass under ammonium in compared with nitrate application, likely due to minimized rhizosphere acidification in agar system (de la Peña Cuao, 2019). While the molecular signaling mechanisms that regulate root:shoot growth in response to N have been examined previously (David et al., 2019; Poitout et al., 2018), our study uncovered different morphological strategies by which Brachypodium maintains the root:shoot ratio in response to different forms of N. Under high ammonium concentrations plants produce a smaller root system but maintain uptake area through increased lateral root formation (Figure 2), while under high nitrate concentrations plants invest in dense root hairs, which have lower energy costs, to maintain N uptake within the smaller root system (Figure 1). Both strategies maintain a functional equilibrium between belowground and aboveground resource acquisition (van Noordwijk et al., 1998; Li et al., 2023).

Ammonium and nitrate have distinct assimilation pathways in plants with different energy requirements (Zayed et al., 2023). Specifically, nitrate assimilation is characterized by energy-intensive reduction steps involving the increased use of NAD(P)H, a byproduct of the TCA cycle, compared to NH_4^+ assimilation (Foyer et al., 2011; Liu and von Wirén, 2017). In our study, the expression of *PEPC1* remains constant across varying ammonium concentrations but increases with increasing nitrate concentration (Figure 7), which likely contributes to the higher energetic demands of NO_3^- assimilation. In maize, increased levels of *PEPC1*, along with phosphoglycerate mutase, suggested an escalation in respiratory metabolism in roots (Prinsi and Espen, 2018). Likewise, the Arabidopsis double mutant *ppc1/ppc2* had severely reduced ammonium and nitrate assimilation under low N concentrations and accumulated more starch and sucrose than wild-type plants grown under nutrient sufficient conditions, suggesting overall decreased energy flux for N assimilation (Shi et al., 2015), which supports our results.

Root growth suppression and aerenchyma formation avoids excessive N accumulation in high N environments

In addition to adjusting enzyme activity to reduce the metabolic cost of N uptake, plants modify root structures at various scales to balance N uptake with energy utilization. At the anatomical scale, under high ammonium concentrations Brachypodium adapts their root energy utilization strategy by reducing the number of living cortical cells and forming aerenchyma in the root cortex. High concentration of ammonium is associated with ethylene production which induces aerenchyma formation (Zhu et al., 2010). However, the observed aerenchyma formation may also be attributed to the expression of the *APs* gene and the programmed cell wall death that results in downstream regulation of the cortex area. This explanation is in accordance with the observation of earlier research that atypical *APs* are involved in reproduction modulated programmed cell wall death in Arabidopsis and rice flowers (Huang et al., 2013; Ge et al., 2005) as explained above.

On the other hand, the root aerenchyma formation could be an adaptive response not only to make an energy balance, but rather a strategy to avoid excessive accumulation of N. Zhang et al. (2007) suggested that root growth suppression at high N concentrations is associated with elevated internal N levels, serving as a mechanism to prevent the excessive accumulation of N in shoot tissue. In our research, however, N concentrations in plant tissue remained relatively stable when media concentrations exceeded 1 mM ammonium or nitrate (Figure 1). We demonstrated that Brachypodium avoids excessive accumulation not only by reducing the root system size but also by down regulating transporters, aquaporins, and possibly through senescence of cortical cells (Figure 5). Earlier studies observed decreased root aerenchyma formation in maize in response to either ammonium and nitrate fertilization (Konings and Verschuren, 1980). On the other hand, it is expected that the root aerenchyma formation could enhance plant growth in N limiting conditions (York et al., 2013). However, our study found that plants grown in high concentrations of ammonium produced aerenchyma in the middle part of their roots (Figure 3). This contrasting findings in low N conditions could be due to early growth stage response of Brachypodium roots to the application of high N concentration. This finding may suggest that aerenchyma formation is not only important for plants under low N conditions but may also play a role in nutrient acquisition under high ammonium conditions. Besides N uptake, this structural change accompanied with the strong transcriptional change could influence the uptake of other nutrients by the root system as well.

N application influences gene expression and nutrient uptake beyond N excessive accumulation

Root anatomical modifications could potentially alter the uptake of nutrients that are otherwise adequately available. Our results highlighted the impact of N application on gene expression beyond those involved in N excessive accumulation. Notably, the transcript levels of *BRADI_1g73970v3*, which encodes the protein SULFUR DEFICIENCY-INDUCED 2, *BRADI_2g38330v3*, associated with zinc ion transmembrane transport, and *BRADI_4g13960v3*, a root-specific metal transporter, are affected by N conditions, with a correlation and potential direct influence on root anatomical changes. Our findings also underscore the complex relationship between sulfur and cysteine metabolism in response to ammonium and nitrate applications. Cysteine, being a key product of sulfur assimilation, plays a crucial role in incorporating sulfur into organic molecules, linking sulfur assimilation directly with N metabolism (Jobe et al., 2019). The upregulation of the sulfur deficiency gene *BRADI_1g73970v3* in higher N concentrations, particularly the moderated response under high ammonium concentrations, indicates a sophisticated sulfur deficiency response. Concurrently, cysteine synthesis, which is critical in plant immunity and cyanide detoxification, showed differential expression patterns depending on the N source, with significant implications for root hair development and plant defense mechanisms (Romero et al., 2014). These findings provide new insights into the complex interplay between nutrient uptake and root structure under varying N conditions, offering potential avenues for enhancing nutrient use efficiency in plants.

Conclusion

Root growth adaptation to N supply is intricately dependent on both the dose and form of N, with distinct root architectural and anatomical responses observed for nitrate and ammonium. Our findings suggest that root growth and physiological responses to N form and concentration are driven by the plant's need to maintain nutrient homeostasis while minimizing metabolic costs. Nitrate supply tends to suppress root growth, possibly as a strategy to optimize nutrient acquisition efficiency. In contrast, ammonium supply results in a more conservative approach, characterized by reduced cortex formation and decreased expression of transporters and aquaporins, reflecting a shift in resource allocation. This dual response highlights the complex regulatory mechanisms plants employ to balance nutrient acquisition with the energetic constraints of high N availability, offering valuable insights for improving nutrient use efficiency in agricultural systems. Understanding these shared genetic pathways can provide valuable insights into breeding strategies aimed at enhancing N use efficiency across a wide range of crops, ultimately contributing to more sustainable agricultural practices.

Data availability statement

RNA-seq data are available in the NCBI SRA under accession number PRJNA1348082 (Brachypodium distachyon, Bd21-3). The data can be accessed at the following link: https://www.ncbi.nlm.nih.gov/bioproject/PRJNA1348082.

Author contributions

HR: Project administration, Methodology, Formal Analysis, Validation, Data curation, Supervision, Writing – original draft, Conceptualization, Software, Writing – review & editing, Visualization, Investigation, Funding acquisition, Resources. DS: Data curation, Formal Analysis, Methodology, Conceptualization, Writing – original draft, Software, Writing – review & editing, Resources, Investigation. CA: Data curation, Software, Formal Analysis, Methodology, Writing – review & editing. BM: Writing – review & editing, Software, Writing – original draft, Data curation, Formal Analysis, Methodology. LS: Writing – original draft, Resources, Investigation, Formal Analysis, Conceptualization, Data curation, Project administration, Writing – review & editing, Methodology, Supervision. BS: Visualization, Methodology, Data curation, Validation, Project administration, Conceptualization, Supervision, Investigation, Software, Funding acquisition, Writing – original draft, Formal Analysis, Resources, Writing – review & editing. AM: Conceptualization, Data curation, Formal Analysis, Funding acquisition, Investigation, Methodology, Project administration, Resources, Software, Supervision, Validation, Visualization, Writing – original draft, Writing – review & editing.

Funding

The author(s) declare financial support was received for the research and/or publication of this article. This work has been funded by the German Research Foundation under Germany's Excellence Strategy, EXC-2070 - 390732324 – PhenoRob. Research reported in the publication was supported by the Foundation for Food & Agriculture Research under award number – Grant ID: 602757 (to AM-C). The content of this publication is solely the responsibility of the authors and does not necessarily represent the official views of the Foundation for Food and Agriculture Research.

Acknowledgments

We sincerely thank Dr. Robert Koller, Dr. Tobias Wojciechowski, and Prof. Uwe Rascher for their invaluable guidance as members of the project advisory board. We are also grateful to Andrea Neuwohner, Sabine Preiskowski, and Prof. Ingar Janzik from IBG-2 for providing lab space and support for RNA extraction from root systems. Special thanks to Kiran Suresh at the

Institute for Cellular and Molecular Botany (IZMB), Bonn University, for assisting with root cross-sections and microscopic imaging. We are also thankful to Dr. Rizwan Riaz and the HOCBio Center at University of Illinois for providing cluster computing access and assistant in bioinformatics analysis.

In memoriam

This work is dedicated to the memory of Prof. Amy Marshall-Colon, who was closely involved in the preparation of this paper and tragically passed away just shortly before its submission. Her name will forever remain in our hearts, not only on the pages of books, but in the lives and souls of the students and colleagues who learned from her how to live with wisdom, humility, and integrity.

Conflict of interest

Author HR was employed by Forschungszentrum Jülich GmbH.

The remaining authors declare that the research was conducted in the absence of any commercial or financial relationships that could be construed as a potential conflict of interest.

Generative AI statement

The author(s) declare that Generative AI was used in the creation of this manuscript. The author(s) verify and take full responsibility for the content of this manuscript. Generative AI (ChatGPT, OpenAI) was used solely to assist with language polishing, grammar correction, and formatting of the text. No AI tools were used for data generation, analysis, or interpretation of results. All scientific content, data, and conclusions presented in this manuscript are the responsibility of the authors.

Any alternative text (alt text) provided alongside figures in this article has been generated by Frontiers with the support of artificial intelligence and reasonable efforts have been made to ensure accuracy, including review by the authors wherever possible. If you identify any issues, please contact us.

Publisher's note

All claims expressed in this article are solely those of the authors and do not necessarily represent those of their affiliated organizations, or those of the publisher, the editors and the reviewers. Any product that may be evaluated in this article, or claim that may be made by its manufacturer, is not guaranteed or endorsed by the publisher.

Supplementary material

The Supplementary Material for this article can be found online at: https://www.frontiersin.org/articles/10.3389/fpls.2025.1708928/full#supplementary-material

References

Asim, M., Ullah, Z., Oluwaseun, A., Wang, Q., and Liu, H. (2020). Signalling overlaps between nitrate and auxin in regulation of the root system architecture: insights from the Arabidopsis thaliana. *Int. J. Mol. Sci.* 21, 2880. doi: 10.3390/ijms21082880

Bray, A. L., and Topp, C. N. (2018). The quantitative genetic control of root architecture in maize. *Plant Cell Physiol.* 59, 1919–1930. doi: 10.1093/pcp/pcy141

Britto, D. T., and Kronzucker, H. J. (2002). NH4+ toxicity in higher plants: a critical review. *J. Plant Physiol.* 159, 567–584. doi: 10.1078/0176-1617-0774

Burton, A. L., Johnson, J., Foerster, J., Hanlon, M. T., Kaeppler, S. M., Lynch, J. P., et al. (2015). QTL mapping and phenotypic variation of root anatomical traits in maize (Zea mays L.). *Theor. Appl. Genet.* 128, 93–106. doi: 10.1007/s00122-014-2414-8

Caburatan, L., and Park, J. (2021). Differential expression, tissue-specific distribution, and posttranslational controls of phosphoenolpyruvate carboxylase. *Plants* 10, 1887. doi: 10.3390/plants10091887

Chen, L.-M., Li, K.-Z., Miwa, T., and Izui, K. (2004). Overexpression of a cyanobacterial phospho enol pyruvate carboxylase with diminished sensitivity to feedback inhibition in Arabidopsis changes amino acid metabolism. *Planta* 219, 440–449. doi: 10.1007/s00425-004-1244-3

Comas, L., Becker, S., Cruz, V. M., Byrne, P. F., and Dierig, D. A. (2013). Root traits contributing to plant productivity under drought. *Front. Plant Sci.* 4. doi: 10.3389/fpls.2013.00442

Cui, X., Wang, J., Li, K., Lv, B., Hou, B., and Ding, Z. (2024). Protein post-translational modifications in auxin signaling. *J. Genet. Genomics* 51, 279–291. doi: 10.1016/j.jgg.2023.07.002

David, L., Girin, T., Fleurisson, E., Phommabouth, E., Mahfoudhi, A., Citerne, S., et al. (2019). Developmental and physiological responses of Brachypodium distachyon to fluctuating nitrogen availability. *Sci. Rep.* 9, 3824. doi: 10.1038/s41598-019-40569-8

de la Peña, M., González-Moro, M. B., and Marino, D. (2019). Providing carbon skeletons to sustain amide synthesis in roots underlines the suitability of Brachypodium distachyon for the study of ammonium stress in cereals. *AoB Plants* 11, plz029. doi: 10.1093/aobpla/plz029

de la Peña Cuao, M. (2019). Brachyodium distachyon as a model for defining the basis of adaptation to ammonium nutrition in grasses.

Drew, M. C., He, C.-J., and Morgan, P. W. (1989). Decreased ethylene biosynthesis, and induction of aerenchyma, by nitrogen-or phosphate-starvation in adventitious roots of Zea mays L. *Plant Physiol.* 91, 266–271. doi: 10.1104/pp.91.1.266

Drew, M. C., He, C.-J., and Morgan, P. W. (2000). Programmed cell death and aerenchyma formation in roots. *Trends Plant Sci.* 5, 123–127. doi: 10.1016/S1360-1385(00)01570-3

Du, Y., and Scheres, B. (2017). Lateral root formation and the multiple roles of auxin. *J. Exp. Bot.* 69, 155–167. doi: 10.1093/jxb/erx223

Du, Y., and Scheres, B. (2018). Lateral root formation and the multiple roles of auxin. *J. Exp. Bot.* 69, 155–167. doi: 10.1093/jxb/erx223

Durinck, S., Spellman, P. T., Birney, E., and Huber, W. (2009). Mapping identifiers for the integration of genomic datasets with the R/Bioconductor package biomaRt. *Nat. Protoc.* 4, 1184–1191. doi: 10.1038/nprot.2009.97

Dziewit, K., Amakorová, P., Novák, O., Szal, B., and Podgórska, A. (2024). Systemic strategies for cytokinin biosynthesis and catabolism in Arabidopsis roots and leaves under prolonged ammonium nutrition. *Plant Physiol. Biochem.*, 213, 108858. doi: 10.1016/j.plaphy.2024.108858

Feria, A. B., Bosch, N., Sánchez, A., Nieto-Ingelmo, A. I., De La Osa, C., Echevarría, C., et al. (2016). Phosphoenolpyruvate carboxylase (PEPC) and PEPC-kinase (PEPC-k) isoenzymes in Arabidopsis thaliana: role in control and abiotic stress conditions. *Planta* 244, 901–913. doi: 10.1007/s00425-016-2556-9

Foyer, C. H., Noctor, G., and Hodges, M. (2011). Respiration and nitrogen assimilation: targeting mitochondria-associated metabolism as a means to enhance nitrogen use efficiency. *J. Exp. Bot.* 62, 1467–1482. doi: 10.1093/jxb/erq453

Galindo-Castañeda, T., Lynch, J. P., Six, J., and Hartmann, M. (2022). Improving soil resource uptake by plants through capitalizing on synergies between root architecture and anatomy and root-associated microorganisms. *Front. Plant Sci.* 13. doi: 10.3389/fpls.2022.827369

Gao, K., Chen, F.-J., Yuan, L.-X., and Mi, G.-H. (2014). Cell production and expansion in the primary root of maize in response to low-nitrogen stress. *J. Integr. Agric.* 13, 2508–2517. doi: 10.1016/S2095-3119(13)60523-7

Gaudin, A. C., Mcclymont, S. A., Holmes, B. M., Lyons, E., and Raizada, M. N. (2011). Novel temporal, fine-scale and growth variation phenotypes in roots of adult-stage maize (Zea mays L.) in response to low nitrogen stress. *Plant Cell Environ.* 34, 2122–2137. doi: 10.1111/j.1365-3040.2011.02409.x

Ge, X., Dietrich, C., Matsuno, M., Li, G., Berg, H., and Xia, Y. (2005). An Arabidopsis aspartic protease functions as an anti-cell-death component in reproduction and embryogenesis. *EMBO Rep.* 6, 282–288. doi: 10.1038/sj.embor.7400357

Giordano, M., Petropoulos, S. A., and Rouphael, Y. (2021). The fate of nitrogen from soil to plants: influence of agricultural practices in modern agriculture. *Agriculture* 11, 944. doi: 10.3390/agriculture11100944

Guo, T., Xuan, H., Yang, Y., Wang, L., Wei, L., Wang, Y., et al. (2014). Transcription analysis of genes encoding the wheat root transporter NRT1 and NRT2 families during nitrogen starvation. *J. Plant Growth Regul.* 33, 837–848. doi: 10.1007/s00344-014-9435-z

Huang, D. W., Sherman, B. T., Tan, Q., Kir, J., Liu, D., Bryant, D., et al. (2007). DAVID Bioinformatics Resources: expanded annotation database and novel algorithms to better extract biology from large gene lists. *Nucleic Acids Res.* 35, W169–W175. doi: 10.1093/nar/gkm415

Huang, J., Zhao, X., Cheng, K., Jiang, Y., Ouyang, Y., Xu, C., et al. (2013). OsAP65, a rice aspartic protease, is essential for male fertility and plays a role in pollen germination and pollen tube growth. *J. Exp. Bot.* 64, 3351–3360. doi: 10.1093/jxb/ert173

Jaramillo, R. E., Nord, E. A., Chimungu, J. G., Brown, K. M., and Lynch, J. P. (2013). Root cortical burden influences drought tolerance in maize. *Ann. Bot.* 112, 429–437. doi: 10.1093/aob/mct069

Jia, Z., Giehl, R. F. H., Meyer, R. C., Altmann, T., and Von Wirén, N. (2019). Natural variation of BSK3 tunes brassinosteroid signaling to regulate root foraging under low nitrogen. *Nat. Commun.* 10, 2378. doi: 10.1038/s41467-019-10331-9

Jia, Z., and von Wirén, N. (2020). Signaling pathways underlying nitrogen-dependent changes in root system architecture: from model to crop species. *J. Exp. Bot.* 71, 4393–4404. doi: 10.1093/jxb/eraa033

Jian-Bo, F., Zhang, Y.-L., Turner, D., Yin-Hua, D., Dong-Sheng, W., and Qi-Rong, S. (2010). Root physiological and morphological characteristics of two rice cultivars with different nitrogen-use efficiency. *Pedosphere* 20, 446–455. doi: 10.1016/S1002-0160(10)60034-3

Jobe, T. O., Zenzen, I., Rahimzadeh Karvansara, P., and Kopriva, S. (2019). Integration of sulfate assimilation with carbon and nitrogen metabolism in transition from C3 to C4 photosynthesis. *J. Exp. Bot.* 70, 4211–4221. doi: 10.1093/jxb/erz250

Kabala, C., Karczewska, A., Gałka, B., Cuske, M., and Sowiński, J. (2017). Seasonal dynamics of nitrate and ammonium ion concentrations in soil solutions collected using MacroRhizon suction cups. *Environ. Monit Assess.* 189, 304. doi: 10.1007/s10661-017-6022-3

Kai, Y., Matsumura, H., and Izui, K. (2003). Phosphoenolpyruvate carboxylase: three-dimensional structure and molecular mechanisms. *Arch. Biochem. Biophys.* 414, 170–179. doi: 10.1016/S0003-9861(03)00170-X

Kazan, K. (2013). Auxin and the integration of environmental signals into plant root development. *Ann. Bot.* 112, 1655–1665. doi: 10.1093/aob/mct229

Kellogg, E. A. (2015). Brachypodium distachyon as a genetic model system. *Annu. Rev. Genet.* 49, 1–20. doi: 10.1146/annurev-genet-112414-055135

Khan, M. I. R., Trivellini, A., Fatma, M., Masood, A., Francini, A., Iqbal, N., et al. (2015). Role of ethylene in responses of plants to nitrogen availability. *Front. Plant Sci.* 6, 161022. doi: 10.3389/fpls.2015.00927

Khramov, D. E., Rostovtseva, E. I., Matalin, D. A., Konoshenkova, A. O., Nedelyaeva, O. I., Volkov, V. S., et al. (2024). Novel proteins of the high-affinity nitrate transporter family NRT2, SaNRT2. 1 and SaNRT2. 5, from the euhalophyte Suaeda altissima: Molecular cloning and expression analysis. *Int. J. Mol. Sci.* 25, 5648. doi: 10.3390/ijms25115648

Klein, S. P., Schneider, H. M., Perkins, A. C., Brown, K. M., and Lynch, J. P. (2020). Multiple integrated root phenotypes are associated with improved drought tolerance. *Plant Physiol.* 183, 1011–1025. doi: 10.1104/pp.20.00211

Koga, N., and Ikeda, M. (1997). Responses to nitrogen sources and regulatory properties of root phosphoenolpyruvate carboxylase. *Soil Sci. Plant Nutr.* 43, 643–650. doi: 10.1080/00380768.1997.10414790

Konings, H., and Verschuren, G. (1980). Formation of aerenchyma in roots of Zea mays in aerated solutions, and its relation to nutrient supply. *Physiologia Plantarum* 49, 265–270. doi: 10.1111/j.1399-3054.1980.tb02661.x

Kumar, N., and Mukhtar, M. S. (2023). Ranking plant network nodes based on their centrality measures. *Entropy* 25, 676. doi: 10.3390/e25040676

Langfelder, P., and Horvath, S. (2008). WGCNA: an R package for weighted correlation network analysis. *BMC Bioinf.* 9, 559. doi: 10.1186/1471-2105-9-559

Lartaud, M., Perin, C., Courtois, B., Thomas, E., Henry, S., Bettembourg, M., et al. (2015). PHIV-RootCell: a supervised image analysis tool for rice root anatomical parameter quantification. *Front. Plant Sci.* 5, 790. doi: 10.3389/fpls.2014.00790

Li, Z., Dou, H., Zhang, W., He, Z., Li, S., Xiang, D., et al. (2023). The root system dominates the growth balance between the aboveground and belowground parts of cotton. *Crop Environ.* 2, 221–232. doi: 10.1016/j.crope.2023.09.001

Lian, L., Lin, Y., Wei, Y., He, W., Cai, Q., Huang, W., et al. (2021). PEPC of sugarcane regulated glutathione S-transferase and altered carbon–nitrogen metabolism under different N source concentrations in Oryza sativa. *BMC Plant Biol.* 21, 287. doi: 10.1186/s12870-021-03071-w

Lima, J., Kojima, S., Takahashi, H., and Wirén, N. (2010). Ammonium triggers lateral root branching in Arabidopsis in an AMMONIUM TRANSPORTER1;3-dependent manner. *Plant Cell* 22, 3621–3633. doi: 10.1105/tpc.110.076216

Liu, Q., Chen, X., Wu, K., and Fu, X. (2015). Nitrogen signaling and use efficiency in plants: what's new? *Curr. Opin. Plant Biol.* 27, 192–198. doi: 10.1016/j.pbi.2015.08.002

Liu, Z., Li, P., Ren, W., Chen, Z., Olukayode, T., Mi, G., et al. (2023). Hybrid performance evaluation and genome-wide association analysis of root system architecture in a maize association population. *Theor. Appl. Genet.* 136, 194. doi: 10.1007/s00122-023-04442-7

Liu, Y., and von Wirén, N. (2017). Ammonium as a signal for physiological and morphological responses in plants. *J. Exp. Bot.* 68, 2581–2592. doi: 10.1093/jxb/erx086

Lynch, J. P. (2019). Root phenotypes for improved nutrient capture: an underexploited opportunity for global agriculture. *New Phytol.* 223, 548–564. doi: 10.1111/nph.15738

Lynch, J. P., Strock, C. F., Schneider, H. M., Sidhu, J. S., Ajmera, I., Galindo-Castañeda, T., et al. (2021). Root anatomy and soil resource capture. *Plant Soil* 466, 21–63. doi: 10.1007/s11104-021-05010-y

Masumoto, C., Miyazawa, S., Ohkawa, H., Fukuda, T., Taniguchi, Y., Murayama, S., et al. (2010). Phosphoenolpyruvate carboxylase intrinsically located in the chloroplast of rice plays a crucial role in ammonium assimilation. *Proc. Natl. Acad. Sci. U.S.A.* 107, 5226–5231. doi: 10.1073/pnas.0913127107

Mazzoni-Putman, S. M., Brumos, J., Zhao, C., Alonso, J. M., and Stepanova, A. N. (2021). Auxin interactions with other hormones in plant development. *Cold Spring Harbor Perspect. Biol.* 13, a039990. doi: 10.1101/cshperspect.a039990

McDonald, M., Galwey, N., and Colmer, T. (2002). Similarity and diversity in adventitious root anatomy as related to root aeration among a range of wetland and dryland grass species. *Plant Cell Environ.* 25, 441–451. doi: 10.1046/j.0016-8025.2001.00817.x

Meier, M., Liu, Y., Lay-Pruitt, K. S., Takahashi, H., and Von Wirén, N. (2020). Auxin-mediated root branching is determined by the form of available nitrogen. *Nat. Plants* 6, 1136–1145. doi: 10.1038/s41477-020-00756-2

Mi, G., Chen, F., Wu, Q., Lai, N., Yuan, L., and Zhang, F. (2010). Ideotype root architecture for efficient nitrogen acquisition by maize in intensive cropping systems. *Sci. China Life Sci.* 53, 1369–1373. doi: 10.1007/s11427-010-4097-y

Miller, A. J., Fan, X., Orsel, M., Smith, S. J., and Wells, D. M. (2007). Nitrate transport and signalling. *J. Exp. Bot.* 58, 2297–2306. doi: 10.1093/jxb/erm066

Naulin, P. A., Armijo, G. I., Vega, A. S., Tamayo, K. P., Gras, D. E., De La Cruz, J., et al. (2019). Nitrate induction of primary root growth requires cytokinin signaling in Arabidopsis thaliana. *Plant Cell Physiol.* 61, 342–352. doi: 10.1093/pcp/pcz199

Nimmo, H. G. (2006). "Control of phosphoenolpyruvate carboxylase in plants," in *Annual Plant Reviews Volume 22: Control of Primary Metabolism in Plants*, Hoboken, New Jersey, USA: Wiley-Blackwell (an imprint of John Wiley & Sons, Inc.). 219–233.

Niu, N., Liang, W., Yang, X., Jin, W., Wilson, Z. A., Hu, J., et al. (2013). EAT1 promotes tapetal cell death by regulating aspartic proteases during male reproductive development in rice. *Nat. Commun.* 4, 1445. doi: 10.1038/ncomms2396

Noguero, M., and Lacombe, B. (2016). Transporters involved in root nitrate uptake and sensing by Arabidopsis. *Front. Plant Sci.* 7. doi: 10.3389/fpls.2016.01391

Orsel, M., Chopin, F., Leleu, O., Smith, S. J., Krapp, A., Daniel-Vedele, F., et al. (2007). Nitrate signaling and the two component high affinity uptake system in Arabidopsis. *Plant Signal Behav.* 2, 260–262. doi: 10.4161/psb.2.4.3870

Pasqualini, S., Ederli, L., Piccioni, C., Batini, P., Bellucci, M., Arcioni, S., et al. (2001). Metabolic regulation and gene expression of root phosphoenolpyruvate carboxylase by different nitrogen sources. *Plant Cell Environ.* 24, 439–447. doi: 10.1046/j.1365-3040.2001.00692.x

Pereira, E. G., Ferreira, L. M., Fernandes, E. D. C., Lima, B. R. D., Santos, L. A., and Fernandes, M. S. (2021). Root morphology and ammonium uptake kinetics in two traditional rice varieties submitted to different doses of ammonium nutrition. *J. Plant Nutr.* 44, 2715–2728. doi: 10.1080/01904167.2021.1927088

Phan, H. A., Iacuone, S., Li, S. F., and Parish, R. W. (2011). The MYB80 transcription factor is required for pollen development and the regulation of tapetal programmed cell death in Arabidopsis thaliana. *Plant Cell* 23, 2209–2224. doi: 10.1105/tpc.110.082651

Poiré, R., Chochois, V., Sirault, X. R., Vogel, J. P., Watt, M., and Furbank, R. T. (2014). Digital imaging approaches for phenotyping whole plant nitrogen and phosphorus response in Brachypodium distachyon. *J. Integr. Plant Biol.* 56, 781–796. doi: 10.1111/jipb.12198

Poitout, A., Crabos, A., Petřík, I., Novák, O., Krouk, G., Lacombe, B., et al. (2018). Responses to systemic nitrogen signaling in Arabidopsis roots involve trans-zeatin in shoots. *Plant Cell* 30, 1243–1257. doi: 10.1105/tpc.18.00011

Prasad, B. D., Creissen, G., Lamb, C., and Chattoo, B. B. (2010). Heterologous expression and characterization of recombinant OsCDR1, a rice aspartic proteinase involved in disease resistance. *Protein Expression Purification* 72, 169–174. doi: 10.1016/j.pep.2010.03.018

Prinsi, B., and Espen, L. (2018). Time-course of metabolic and proteomic responses to different nitrate/ammonium availabilities in roots and leaves of maize. *Int. J. Mol. Sci.* 19:2202. doi: 10.3390/ijms19082202

Raudvere, U., Kolberg, L., Kuzmin, I., Arak, T., Adler, P., Peterson, H., et al. (2019). g: Profiler: a web server for functional enrichment analysis and conversions of gene lists, (2019 update). *Nucleic Acids Res.* 47, W191–W198. doi: 10.1093/nar/gkz369

Ravazzolo, L., Trevisan, S., Manoli, A., Boutet-Mercey, S., Perreau, F., and Quaggiotti, S. (2019). The control of zealactone biosynthesis and exudation is involved in the response to nitrogen in maize root. *Plant Cell Physiol.* 60, 2100–2112. doi: 10.1093/pcp/pcz108

R Core Team (2013). *R: A language and environment for statistical computing*. (Vienna, Austria: R Foundation). Available online at: http://www.r-project.org/"www.R-project.org/ (Accessed August 22, 2025).

Rogers, E. D., and Benfey, P. N. (2015). Regulation of plant root system architecture: implications for crop advancement. *Curr. Opin. Biotechnol.* 32, 93–98. doi: 10.1016/j.copbio.2014.11.015

Rogg, L. E., and Bartel, B. (2001). Auxin signaling: derepression through regulated proteolysis. *Dev. Cell* 1, 595–604. doi: 10.1016/S1534-5807(01)00077-6

Romero, L. C., Aroca, M.Á., Laureano-Marín, A. M., Moreno, I., García, I., and Gotor, C. (2014). Cysteine and cysteine-related signaling pathways in Arabidopsis thaliana. *Mol. Plant* 7, 264–276. doi: 10.1093/mp/sst168

Rubio-Asensio, J. S., López-Berenguer, C., García-De La Garma, J., Burger, M., and Bloom, A. J. (2014). "Root strategies for nitrate assimilation," in *Root Engineering: basic and applied concepts* (Berlin, Heidelberg: Springer Berlin Heidelberg).

Saengwilai, P., Nord, E. A., Chimungu, J. G., Brown, K. M., and Lynch, J. P. (2014a). Root cortical aerenchyma enhances nitrogen acquisition from low-nitrogen soils in maize. *Plant Physiol.* 166, 726–735. doi: 10.1104/pp.114.241711

Saengwilai, P., Tian, X., and Lynch, J. P. (2014b). Low crown root number enhances nitrogen acquisition from low-nitrogen soils in maize. *Plant Physiol.* 166, 581–589. doi: 10.1104/pp.113.232603

Schaarschmidt, S., Fischer, A., Zuther, E., and Hincha, D. K. (2020). Evaluation of seven different RNA-seq alignment tools based on experimental data from the model plant Arabidopsis thaliana. *Int. J. Mol. Sci.* 21, 1720. doi: 10.3390/ijms21051720

Shi, J., Yi, K., Liu, Y., Xie, L., Zhou, Z., Chen, Y., et al. (2015). Phosphoenolpyruvate carboxylase in Arabidopsis leaves plays a crucial role in carbon and nitrogen metabolism. *Plant Physiol.* 167, 671–681. doi: 10.1104/pp.114.254474

Sigalas, P. P., Buchner, P., Kröper, A., and Hawkesford, M. J. (2024). The functional diversity of the high-affinity nitrate transporter gene family in hexaploid wheat: insights from distinct expression profiles. *Int. J. Mol. Sci.* 25, 509. doi: 10.3390/ijms25010509

Simões, I., and Faro, C. (2004). Structure and function of plant aspartic proteinases. *Eur. J. Biochem.* 271, 2067–2075. doi: 10.1111/j.1432-1033.2004.04136.x

Soares, A., Niedermaier, S., Faro, R., Loos, A., Manadas, B., Faro, C., et al. (2019). An atypical aspartic protease modulates lateral root development in Arabidopsis thaliana. *J. Exp. Bot.* 70, 2157–2171. doi: 10.1093/jxb/erz059

Su, T., Yang, M., Wang, P., Zhao, Y., and Ma, C. (2020). Interplay between the ubiquitin proteasome system and ubiquitin-mediated autophagy in plants. *Cells* 9, 2219. doi: 10.3390/cells9102219

Sun, H., Xu, F., Guo, X., Wu, D., Zhang, X., Lou, M., et al. (2019). A strigolactone signal inhibits secondary lateral root development in rice. *Front. Plant Sci.* 10, 1527. doi: 10.3389/fpls.2019.01527

Tian, Q., Chen, F., Zhang, F., and Mi, G. (2005). Possible involvement of cytokinin in nitrate-mediated root growth in maize. *Plant Soil* 277, 185–196. doi: 10.1007/s11104-005-6837-5

Tognetti, V. B., Mühlenbock, P., and Van Breusegem, F. (2012). Stress homeostasis–the redox and auxin perspective. *Plant Cell Environ.* 35, 321–333. doi: 10.1111/j.1365-3040.2011.02324.x

Trachsel, S., Kaeppler, S. M., Brown, K. M., and Lynch, J. P. (2013). Maize root growth angles become steeper under low N conditions. *Field Crops Res.* 140, 18–31. doi: 10.1016/j.fcr.2012.09.010

van der Hoorn, R. A. (2008). Plant proteases: from phenotypes to molecular mechanisms. *Annu. Rev. Plant Biol.* 59, 191–223. doi: 10.1146/annurev.arplant.59.032607.092835

van Noordwijk, M., Martikainen, P., Bottner, P., Cuevas, E., Rouland, C., and Dhillion, S. S. (1998). Global change and root function. *Global Change Biol.* 4, 759–772. doi: 10.1046/j.1365-2486.1998.00192.x

Vidmar, J. J., Zhuo, D., Siddiqi, M. Y., Schjoerring, J. K., Touraine, B., and Glass, A. D. (2000). Regulation of high-affinity nitrate transporter genes and high-affinity nitrate influx by nitrogen pools in roots of barley. *Plant Physiol.* 123, 307–318. doi: 10.1104/pp.123.1.307

Vierstra, R. D. (2009). The ubiquitin–26S proteasome system at the nexus of plant biology. *Nat. Rev. Mol. Cell Biol.* 10, 385–397. doi: 10.1038/nrm2688

Wang, M., Ding, L., Gao, L., Li, Y., Shen, Q., and Guo, S. (2016). The interactions of aquaporins and mineral nutrients in higher plants. *Int. J. Mol. Sci.* 17, 1229. doi: 10.3390/ijms17081229

Wang, H., Wang, Z., and Dong, X. (2019). Anatomical structures of fine roots of 91 vascular plant species from four groups in a temperate forest in Northeast China. *PloS One* 14, e0215126. doi: 10.1371/journal.pone.0215126

Xiaoli, N., Hanmi, Z., Xiukang, W., Tiantian, H., Puyu, F., Ting, L., et al. (2020). Changes in root hydraulic conductance in relation to the overall growth response of maize seedlings to partial root-zone nitrogen application. *Agric. Water Manage.* 229, 105839. doi: 10.1016/j.agwat.2019.105839

York, L. M., Nord, E., and Lynch, J. (2013). Integration of root phenes for soil resource acquisition. *Front. Plant Sci.* 4, 355. doi: 10.3389/fpls.2013.00355

Yu, G., Wang, L. G., Han, Y., and He, Q. Y. (2012). clusterProfiler: an R package for comparing biological themes among gene clusters. *Omics* 16, 284–287. doi: 10.1089/omi.2011.0118

Zayed, O., Hewedy, O. A., Abdelmoteleb, A., Ali, M., Youssef, M. S., Roumia, A. F., et al. (2023). Nitrogen journey in plants: from uptake to metabolism, stress response, and microbe interaction. *Biomolecules* 13, 1443. doi: 10.3390/biom13101443

Zhang, H., Rong, H., and Pilbeam, D. (2007). Signalling mechanisms underlying the morphological responses of the root system to nitrogen in Arabidopsis thaliana. *J. Exp. Bot.* 58, 2329–2338. doi: 10.1093/jxb/erm114

Zhiyong, Z., Baomin, F., Chao, S., Xiaoxian, Z., Qingwen, Z., and Bing, Y. (2022). Advances in root system architecture: functionality, plasticity, and research methods. *J. Resour. Ecol.* 14, 15–24. doi: 10.5814/j.issn.1674-764x.2023.01.002

Zhu, J., Brown, K. M., and Lynch, J. P. (2010). Root cortical aerenchyma improves the drought tolerance of maize (Zea mays L.). *Plant Cell Environ.* 33, 740–749. doi: 10.1111/j.1365-3040.2009.02099.x

Zotarelli, L., Scholberg, J. M., Dukes, M. D., and Muñoz-Carpena, R. (2007). Monitoring of nitrate leaching in sandy soils: comparison of three methods. *J. Environ. Qual.* 36, 953–962. doi: 10.2134/jeq2006.0292